Interaction of HIF and USF signaling pathways at human genes flanked by hypoxia-response elements and E-box palindromes

Hu, J ; Stiehl, D P ; Setzer, C ; Wichmann, D ; Shinde, D A ; Rehrauer, H ; Hradecky, P ; Gassmann, M ; Gorr, T A

Abstract: Rampant activity of the hypoxia-inducible factor (HIF)-1 in cancer is frequently associated with the malignant progression into a harder-to-treat, increasingly aggressive phenotype. Clearly, anti-HIF strategies in cancer cells are of considerable clinical interest. One way to fine-tune, or inhibit, HIF's transcriptional outflow independently of hydroxylase activities could be through competing transcription factors. A CACGTG-binding activity in human hepatoma cells was previously found to restrict HIF's access to hypoxia response cis-elements (HRE) in a Daphnia globin gene promoter construct (phb2). The CACGTG factor, and its impact on hypoxia-responsive human genes, was analyzed in this study by genome-wide computational scans as well as gene-specific quantitative PCR, reporter and DNA-binding assays in hepatoma (Hep3B), cervical carcinoma (HeLa), and breast carcinoma (MCF7) cells. Among six basic helix-loop-helix transcription factors known to target CACGTG palindromes, we identified upstream stimulatory factor (USF)-1/2 as predominant phb2 CACGTG constituents in Hep3B, HeLa, and MCF7 cells. Human genes with adjacent or overlapping HRE and CACGTG motifs included with lactate dehydrogenase A (LDHA) and Bcl-2/E1B 19 kDa interacting protein 3 (BNIP3) hypoxia-induced HIF-1 targets. Parallel recruitment of HIF-1 and USF1/2a to the respective promoter chromatin was verified for all cell lines investigated. Mutual complementing (LDHA) or moderating (BNIP3) cross-talk was seen upon overexpression or silencing of HIF-1 and USF1/2a. Distinct (LDHA) or overlapping (BNIP3) promoter-binding sites for HIF-1 and USFs were subsequently characterized. We propose that, depending on abundance or activity of its protein constituents, O(2)-independent USF signaling can function to fine-tune or interfere with HIF-mediated transcription in cancer cells. Mol Cancer Res; 1-17.

DOI: https://doi.org/10.1158/1541-7786.MCR-11-0090

Interaction of HIF and USF signaling pathways at human genes flanked by hypoxia-response elements and E-box palindromes

Junmin Hu[1], Daniel P. Stiehl[2], Claudia Setzer[1], Daniela Wichmann[1], Dheeraj A. Shinde[1], Hubert Rehrauer[3], Pavel Hradecky[4], Max Gassmann[1,5], Thomas A. Gorr[1,6]

[1] Institute of Veterinary Physiology, University of Zurich, Zurich, Switzerland

[2] Institute of Physiology, University of Zurich, Zurich, Switzerland

[3] Functional Genomics Center Zurich, Zurich, Switzerland

[4] AltraBio, Lyon, France

[5] Zurich Center for Integrative Human Physiology (ZIHP), Zurich, Switzerland

[6] Center for Pediatrics and Adolescent Medicine, University Medical Center Freiburg, Freiburg, Germany

Running title: HIF-USF interaction

Total word count: 9634 (including abstract, references)

Total character count (excluding spaces): 55746 (including abstract, references)

*** corresponding author:** Thomas A. Gorr, PhD

Institute of Veterinary Physiology, Vetsuisse Faculty, University of Zurich,

Winterthurerstrasse 260, 8057 Zurich, Switzerland

💻 tgorr@access.uzh.ch ☎ +41 (0)44 635 8807 🖹 +41 (0)44 635 8932

Abstract

Rampant activity of the hypoxia-inducible factor HIF-1 in cancer is frequently associated with the malignant progression into a harder-to-treat, increasingly aggressive phenotype. Clearly, anti-HIF strategies in cancer cells are of considerable clinical interest. One way to fine-tune, or inhibit, HIF's transcriptional outflow independently of hydroxylase activities could be through competing transcription factors. A CACGTG-binding activity in human hepatoma cells was previously found to restrict HIF's access to hypoxia response *cis*-elements (HREs) in a *Daphnia* globin gene promoter construct (phb2). The CACGTG-factor, and its impact on hypoxia-responsive *human* genes, was analyzed in this study using genome-wide computational scans as well as gene specific quantitative PCR, reporter and DNA binding assays in hepatoma (Hep3B), cervical carcinoma (HeLa) and breast carcinoma (MCF7) cells. Among six basic helix-loop-helix transcription factors known to target CACGTG palindromes, we identified upstream stimulatory factor (USF)-1/2 as predominant phb2 CACGTG-constituents in Hep3B, HeLa and MCF7 cells. Human genes with adjacent or overlapping HRE and CACGTG motifs included with lactate dehydrogenase A (LDHA) and Bcl-2/E1B 19 kDa interacting protein 3 (BNIP3) hypoxia-induced HIF-1 targets. Parallel recruitment of HIF-1α and USF1/2a to the respective promoter chromatin was verified for all cell lines investigated. Mutual complementing (LDHA) or moderating (BNIP3) crosstalk was seen upon over-expression or silencing of HIF-1α and USF1/2a. Distinct (LDHA) or overlapping (BNIP3) promoter-binding sites for HIF-1 and USFs were subsequently characterized. We propose that, depending on abundance or activity of its protein constituents, O_2-independent USF signaling can function to fine-tune or interfere with HIF-mediated transcription in cancer cells.

Introduction

Relaying minutes-to-hours of inadequate oxygenation (hypoxia) onto the level of DNA via the hypoxia inducible transcription factors 1 and 2 (HIF-1 and -2) is a highly conserved signaling event across the animal kingdom (1, 2). When exposed to low oxygen partial pressures (pO_2), the mammalian HIF-1/-2 complexes function as heterodimer of HIF-1α or -2α and HIF-1β subunits (3, 4). Whereas HIF-1β, also known as ARNT (aryl hydrocarbon receptor nuclear translocator), is constitutively present, the activity and abundance of HIF-α subunits are regulated as a function of pO_2. In the presence of oxygen homologs of prolyl hydroxylase domain 1-3 (PHD1-3) dioxygenases catalyze the Fe (II)-dependent hydroxylation of two proline residues contained within the oxygen-dependent degradation (ODD) domain and the N-terminal transactivation domain (NAD; rear proline only) of HIF-1α and -2α (5-7). Once prolyl hydroxylated, HIF-α subunits are captured by the von Hippel-Lindau tumor suppressor protein (VHL) and rapidly degraded via the ubiquitin-proteasome pathway (6, 8). A second, O_2-requiring post-translational modification of HIF-1α/-2α targets a single asparagine residue within the subunits` C-terminal transactivation domain (CAD). It is catalyzed by asparaginyl hydroxylase called factor inhibiting HIF-1 (FIH-1) to prohibit HIF-α:co-activator interaction and suppress trans-activation of genes under high oxygen (9, 10). During hypoxia, both PHD and FIH-1 activities are progressively inhibited, leading to α-subunit accumulation, α:β-subunit dimerization in the nucleus and binding of the heterodimer to hypoxia response element (HRE) within target genes. Being members of canonical CANNTG E-box motifs, HREs consist of a consensus 5'-VNVBRCGTG-3' (11) (V=not T; N=any; B=not A; R=A or G). To date, several hundred potential (12) and more than 70 validated (11) hypoxia-responsive and HRE-flanked gene targets of HIF-1 have been identified. Through this transcriptional outflow, HIF-1 is able to reprogram cellular metabolism, growth, apoptosis, and O_2 supply in response to declining pO_2 (11).

Non-redundant roles of these hydroxylase systems in the regulation of HIF-1α/-2α activities were only recently unraveled when it became clear that the Michaelis constant (K_m) of all three PHDs and FIH-1 predicted a distinctly lower oxygen affinity for the former (13). Consequently, PHD1-3 hydroxylases start to experience, relative to FIH-1, inactivation at higher pO_2 during progressing hypoxia (14). Differential hydroxylase activities will eventually translate into a differential regulation of HIF-1 targets. By combining transcriptional profiling data (15) with a numerical model of the regulatory dynamics of the FIH-1 and PHD oxygen sensors along a virtual oxygen gradient (16), Pouysségur and colleagues were able to allocate HIF-1 targets into two categories: i) FIH-1 inhibited genes, i.e. those induced by progressive hypoxia once the NAD and, subsequently, CAD of HIF-1α/-2α are both released from inhibition (e.g. CA9, PHD3, LDHA), and ii) non-FIH-1 inhibited genes, i.e. those requiring solely HIF-α NAD activity upon sufficient PHD inhibition while being refractory to any CAD activation (e.g. PGK1, GAPDH) (15, 17). This categorization predicts expression of FIH-1 inhibited genes to be altered during severe hypoxia, whereas moderate degrees of O_2 deprivation already affect non-FIH-1 inhibited genes.

Yet, as another and hydroxylase-independent layer of control, HIF's transcriptional outflow is also prone to be influenced by competing transcription factors. When we previously utilized reporter constructs of the tripartite globin-2 gene (hb2) promoter (phb2) of the planktonic crustacean *Daphnia magna* in heterologous transfections of human cancer cells we noticed a constitutive CACGTG-binding factor which was able to interfere with the HIF-1-driven induction of the phb2 luciferase reporter (18). Now, we identify this phb2 CACGTG factor across several cancer cell lines as a complex of O_2-independently acting upstream stimulatory factors 1 and 2 (USF1, USF2). To assess both the extent and mode (positive/negative) of the impact of USF-signaling on HIF's transcriptional outflow, we implemented a genome-wide computational scan to identify candidate *human* genes that contain adjacent or overlapping HRE and CACGTG palindrome motifs in their up- or downstream sequences. Our results suggest the occurrence both of positive (promoter of lactate dehydrogenase A, LDHA: USFs complement HIF control)

and variably negative (promoter of Bcl-2/E1B 19 kDa interacting protein 3, BNIP3: USFs interactions range from moderating to competing with HIF-1) crosstalk modes when HIF-1/USF constituents were over-expressed or silenced. The current work, therefore, provides a proof-of-principle study for the oxygen-independent USF pathway to influence, and, upon strong activation or over-expression, even inhibit HIF/HRE-mediated gene expression in human cancer cells.

Materials and Methods

Cells, RNA and quantitative PCR (qPCR): Human hepatoma (Hep3B; ATCC HB-8064), cervical carcinoma (HeLa; ATCC CCL-2) and breast carcinoma cells (MCF7; ATCC HTB-22) were purchased as short tandem repeat (STR)-authenticated lines from the American Tissue Culture Collection (ATCC) and maintained in high glucose (4.5g/l) Dulbecco's modified Eagle's medium (DMEM) as described earlier (18). Normoxic cultures: 37°C, room air in water-saturated atmosphere with 5% CO_2 (i.e. a pO_2 = 141.6 mmHg, [O_2] = 18.6% O_2). Hypoxic cultures in HERA Cell240 incubator (Heraeus) or a polymer glove box (Coy) – 16h exposures: 37°C, in water-saturated 1% O_2/5% CO_2/balance N_2 atmosphere. Isolation of total RNA, reverse transcriptions and SYBR-Green qPCR were carried out as previously reported (19, 20). All primers used for qPCR are listed in Supplement Table 1, ST1.

Antibodies: Mouse monoclonal anti-ATF-1 antibody (25C10G, sc-270) and rabbit polyclonal anti-USF1 (C-20, sc-229) were purchased from Santa Cruz Biotech, INC. Rabbit polyclonal anti-USF1M, anti-USF2F, anti-USF2G, anti-USF2Z and anti-USF2aO antibodies were kindly provided by Dr. B. Viollet (21). Additional antibody gifts included: a) rabbit anti human DEC1 (CW27) (22); b) rabbit anti human MYC (23); c) rabbit anti mouse ARNT (anti-mARNT R-1 lgG) (24); d) rabbit anti human ARNT (anti-hARNT C34) (25); e) rabbit anti human USF full length antibody (USF FL) (26).

Sequence scan for HRE motif and CACGTG palindrome: We used the repeat-masked human genome sequence as provided by the UCSC Genome Bioinformatics Website (Version hg19, GRCh37) at http://hgdownload.cse.ucsc.edu/goldenPath/hg19/bigZips/chromFaMasked.tar.gz. Gene definitions and transcription start sites were from http://hgdownload.cse.ucsc.edu/goldenPath/hg19/database/refGene.txt.gz (downloaded April 09, 2010). The search for motifs, implemented as R-script, was conducted among the 1000 base flanking region up- and downstream (= ±1000 bp) of annotated transcripts. Genes containing both HRE and CACGTG palindrome motifs within the ±1000 bp flanks were only considered as HRE/palindrome gene if the motif-motif distance ≤ 100 bp. Based on these criteria, we used the GeneGo MetaCore system to identify pathways where HRE/ palindrome genes are overrepresented (see Table 1).

Luciferase reporter: Using genomic DNA, we amplified the promoter region around the HRE and E-box palindrome motifs via nested PCR (for primers, see Suppl. Table ST1**)**. Of note, the 3'-end of any given amplicon always extended into the first coding exon of the respective gene. In detail, we amplified and cloned the following promoter regions (start/end always relative to translation start ATG codon): a) human 4EBP1 gene, -518/+403; b) human MC1R gene, -880/+9; c) human LDHA gene, -2617/+530; d) human TYR gene, -400/+108. Following TOPO-cloning of the PCR products into the pCRII-TOPO vector (Invitrogen), the liberated insert was ligated into pGL3-basic luciferase vector (Promega AG, Dübendorf, Switzerland) to generate the luciferase reporter constructs. We also obtained the BNIP3/pGL3-basic (-753/+3) (27) and the PHD2/pGL3-basic (-607/+3) (28) luciferase reporter vector as kind gifts. HIF-1α (i.e. pcDNA3.1-hHIF-1-PK tag) as well as USF (pCR3-USF1, pCR3-USF2a and pCR3-USF2b) expression plasmids were generously supplied by Prof. P. Maxwell (29) and Dr. B. Viollet (30), respectively.

*Electrophoretic Mobility Shift Assay (EMSA) and Pull-down assay***:** Isolation of nuclear protein extracts of Hep3B, HeLa and MCF7 cells, and analysis of *in vitro* protein-DNA interaction by EMSA (18) and pull-down assays (31), was done as previously reported. All oligonucleotide sequences used as probes for

either assay are shown in Supplementary Table ST1. For EMSA gel supershifts, 1.0-1.5 μl of rabbit anti-USF1M, rabbit anti-USF2G or mouse anti-HIF-1α (mgc3) was added into the reaction (30 min, room temperature). Negative supershift controls included 1.5 μl pre-immune serum from the same rabbit to be immunized against USF1M or USF2G, as well as 1.0 μl rabbit anti-human IgG (code: 309-005-003 Jackson Immuno Research). Regarding pull-down assays, wildtype and mutated phb2 -146 palindrome or -107 HRE oligonucleotides, and wildtype and mutated BNIP3 -251/-246 HRE oligonucleotides, biotinylated at the 5' end and PAGE purified, were annealed into double stranded DNA and immobilized on streptavidin-coated magnetic beads (Dynal Biotech, Oslo, Norway) as described (31).

Western blot and co-immunoprecipitation: Proteins were resolved in 10% SDS polyacrylamide gels, transferred onto nitrocellulose membranes (Whatman GmbH, Germany), and the membranes incubated at 4°C overnight with the following primary antibodies diluted in 5% milk TBS-T: (a) anti-HIF1α (mgc3) (1:500) or (b) anti-USF1M or anti-USF2G (1:750). The signal was detected with horseradish peroxidase-conjugated goat anti-mouse or anti-rabbit (1:5000) and luminol substrate. For Co-IP experiments, 150 μg nuclear protein was incubated with 20 μl mouse anti-HIF-1α or 0.75 μg anti-mARNT or 2.5 μl USF antiserum and subsequently rotated at 4°C overnight. The next day, 40 μl of protein G beads were added into the mix and incubated at 4°C for another 2.5h. The extract/antibody/bead mix was collected by centrifugation, the pellet boiled at 95°C in 1×SDS sample buffer for 10min and the supernatant analyzed by Western blot.

Chromatin Immunoprecipitation (ChIP) assay: ChIP assays were performed in human Hep3B, HeLa and MCF7 cells after a 4h exposure to normoxic (air) or hypoxic (1% O_2) atmospheres as described (32). In brief, genomic DNA was crosslinked with bound proteins (10 min, room temperature) using 1% formaldehyde in 1× phosphate-buffered saline (PBS) and sonicated in a Bioruptor™ UCD-200 (Diagenode sa, Liège, Belgium) or a Sonifier cell disruptor B15 (Branson) into 500-1000 bp fragments.

For immunoprecipitation of the DNA:protein mix, 4.5 μl rabbit polyclonal anti-HIF-1α IgG (ab2185, Abcam, Cambridge, UK), 10 μl rabbit polyclonal anti-USF1M or anti-USF2G was added into the chromatin solution. 10 μl pre-immune rabbit antiserum and 2.5 μl rabbit anti-human IgG were used as negative controls. The purified DNA was amplified by PCR using the ChIP primer pairs shown in Supplementary Table ST1.

Transient luciferase reporter transfection: Half-confluent Hep3B, HeLa and MCF7 cells were transfected overnight using the calcium phosphate method with different luciferase (LUC) reporter constructs and normalization plasmids expressing β–galactosidase. For co-transfections, 15-500ng HIF-1α plasmid and/or 15-100ng USF1, USF2a or USF2b plasmid were added. In each transfection, pUC18 plasmid was used as filler DNA for a total of 2-3μg DNA. The following day, each batch of transfected cells was split in two for parallel 16h normoxia (N) and hypoxia (H) exposure. After 16h N/H exposure cells were lysed and LUC activity was measured using a commercially available Luciferase Assay System (Promega AG) and a SIRIUS Luminometer (Berthold Technologies, Germany). LUC activity was normalized by β-galactosidase activity (β-galactosidase enzyme assay kit; Promega AG) and expressed as "relative luciferase activity" in percent (% RLA) of the total activity of all normoxic and hypoxic reactions of a given assay.

Transient knockdown of HIF-1α, USF1 or USF2a: For transient silencing, the specific siRNA HIF-1α and siRNA USF1 oligonucleotides were selected based on previous publications (33-35). All siRNA sequences (see Suppl. Table ST1) were synthesized by Dharmacon Research Inc. Si*CONTROL* non-targeting siRNA pool #2 was used as scrambled siRNA control (Dharmacon). Half-confluent Hep3B cells were transfected with a total of 200nM of siRNAs using Oligofectamine™ reagent (Invitrogen). In the combined USF1+USF2a siRNA transfection targeting both USFs, 100nM of each siRNA were added to the cells.

Statistics: Using STATA 10.0 software (Stata™ 10.0; StataCorp, USA) we compared control-vs.-experimental mean transcript expression levels (Fig. 3) and relative luciferase activities (RLA) for each reporter assay (Fig. 6) within the *same* oxygen category (either normoxic or hypoxic results; Figs. 3 and 6) or for the hypoxic/normoxic fold inductions (Fig. 3, Table 3). In accordance with prior testing for normality of data populations and for equal variances between samples, statistical significance (i.e. p value < 0.05) was calculated by i) one-way Anova/post-hoc Sidak modeling (normality/variance equality both maintained) or Welch-approximated t-tests in case of unequal sample variances (e.g. Fig. 6B, C; *used symbols:* ∗; +), and ii) non-parametric Kruskal-Wallis tests plus Wilcoxon rank-sums for pairwise sample comparisons when both assumptions were violated (e.g. Fig. 3 and Fig. 6A, D; *used symbols*: #; ¶).

Results

CACGTG palindromic E-boxes often serve as binding sites for several non-HIF basic helix-loop-helix (bHLH) transcription factors, including ARNT (36, 37), MYC (38, 39), USFs (21), STRA13/DEC1 (22), ATF-1 and CREB-1 (40). To identify the factor(s) responsible for the HIF-interfering constitutive activity at the -146 CACGTG element within the promoter of the hb2 gene (phb2) of *Daphnia magna* (18), and map the factor(s) occurrence across different cancer cells, we conducted an EMSA survey using normoxic nuclear extracts from human hepatoma (Hep3B), cervical carcinoma (HeLa) and breast carcinoma cells (MCF7). Since HeLa and MCF7 EMSA screens yielded compatible results, **Figure 1A** presents Hep3B data only (Fig. 1A). The protein components within the constitutive complex (cc) of the -146 phb2 binding activity were identified using specific antibodies directed against USFs, DEC1, MYC, ARNT and ATF-1. Of these five factors screened by supershifts (ss), only USF1 and USF2 were recognized as main *in vitro* binding factors of the -146 phb2 palindrome (Fig. 1A, lanes 3, 5, 7, 9, 11) while all other factors either failed (MYC, ATF-1) binding this motif or interacted (DEC1) weakly with it (Fig. 1A, lane 15; ~5-

10% of total pool). The preponderance of USFs as protein components in the HIF-interfering complex of *Daphnia*`s hb2 promoter prompted us to subsequently focus on this transcription factor family. Increasing the volume of anti-USF1M (left) and anti-USF2G (right) antiserum in the binding reaction nuclear extracts from normoxic (N) and hypoxic (H) Hep3B reduced the intensity of the CACGTG complex in a dose-dependent manner (Suppl. Fig. S1A). Binding of USF proteins to the -146 phb2 E-box was clearly oxygen-independent (Fig. S1A).

We re-evaluated our EMSA results through independent pull-down assays of Hep3B, HeLa and MCF7 nuclear proteins using biotinylated phb2 oligonucleotides, bound to streptavidin coated magnetic beads. In a representative assay with HeLa normoxic (N) and hypoxic (H) nuclear extracts (Fig. 1B+C), wildtype biotinylated oligonucleotides (w-bio), containing the -146 CACGTG phb2 palindrome, were able to pull down 43 kDa USF1 (Fig. 1B), 44 kDa USF2a and 38 kDa USF2b proteins in an oxygen-independent manner (Fig. 1C). In support of a specific interaction, competition assays (50× comp. lanes) or beads coated with -146 mutant (m-bio) E-box motifs (5'-CAATGT-3') greatly reduced or abolished the USF pull-down. Similar results were obtained with extracts from Hep3B and MCF7 cells (not shown). Further pull-down and co-immunoprecipitation analyses verified that i) USF1/2 (CACGTG preference) and HIF-1 complexes (TACGTG preference) display high-affinity binding to distinct elements within phb2, and ii) the USF-HIF interference within phb2 is DNA context dependent, since we, and others (41), could not detect any direct physical interaction between USFs and HIF subunits (see Suppl. Fig. S1B-E).

To move beyond the *Daphnia* hb2 promoter as a model for occurring crosstalk among E-box complexes, we adopted *Daphnia* phb2 coordinates to conduct a genome-wide screen and enrichment analysis for *human* genes that harbor, within 1000 bases from their transcriptional frame (in up- and downstream direction), both a 5'-VNVBRCGTG-3' HRE consensus motif (11) and a 5'-CACGTG-3' palindrome with a motif-motif distance of ≤ 100bp. According to these criteria, our survey found multiple examples of known HIF targets among the list of HRE/palindrome genes including vascular endothelial growth factor

C (VEGFC), lactate dehydrogenase A (LDHA), phosphoglucomutase 2 (PGM2), enolase 1 (ENO1), transferrin (TF), eukaryotic translation initiation factor 4E binding protein 1 (4EBP1), Bcl-2/E1B 19 kDa interacting protein 3-like (BNIP3L) and Bcl-2–associated X protein (BAX) (an *Excel file with the detected human HRE/palindrome candidate genes is available upon request*). When we looked at the top-scoring GeneGo pathways, whose signaling components showed a highly significant enrichment of HRE/palindrome genes (see **Table 1**), we noticed several signal transductions where USFs appear to impinge on hypoxia signals in a highly localized manner (e.g. insulin-regulated/cap-dependent mRNA translation, HIF mediated transcription and cytoskeletal or cell cycle control functions). Interestingly, particular focal points of HRE/palindrome gene clusters included the eIF4F checkpoint of cap-dependent translation control, cell surface receptors for insulin and growth factors as well as actin remodeling genes (see Table 1; Gene Symbols). These pathway aggregations of possibly co-regulated genes inspired the current study to try and provide solid proof-of-principle for a USF-based modulation of, or interference with, the HIF transcriptional outflow for at least some of the known targets listed above. If successful, future work will need to comprehensively assess USF-HIF cross-talk in cancer cells in a physiological context (see discussion).

For initial insights on HIF/USF-convergence at DNA level we i) established those genes with a strong human-mouse-rat (hmr) conservation of the HRE/palindrome motifs within the aligned promoter regions (**Table 2;** Suppl. Fig. S2), and ii) examined the mRNA expression of five such hmr-conserved HRE/palindrome candidates by quantitative real-time PCR (qPCR) in conjunction with transient, small-interfering RNA (siRNA)-based knockdowns of HIF-1α, USF1 and USF2a in Hep3B (see **Fig. 2** for knockdown efficacy assessment by Western blot). Transfection with scrambled (scr) RNA did not affect steady state abundance of HIF-1α, USF1 and USF2a proteins (scr; compare to non-transfected (non-TF) cells). In contrast, exposing Hep3B cells to siRNAs specifically directed against HIF-1α (siHIF-1α), USF1 (siUSF1), USF2a (siUSF2a) or the combination of both USFs (siUSF1/2a) resulted in a drastically

diminished expression of the respective factor(s). In cells subjected to a USF1 knockdown (siUSF1), effects on the expression of USF2a ranged from unaltered to a slight elevation. Conversely, silencing of USF2a (siUSF2a) was accompanied by a strong reduction of USF1 protein level (Fig. 2, USF1 signal in siUSF2a). Similar to these findings, both USFs were concomitantly lost in USF2 knockout mouse models, suggesting USF2 to be generally required as USF1 trans-activator (42).

Following transient knockdown of HIF-1 and USFs in normoxic and hypoxic Hep3B cells, changes in mRNA levels of the HRE/palindrome candidates LDHA, BNIP3, BNIP3L, 4EBP1 and VEGFC were assessed by qPCR **(Fig. 3)**. Transcripts of BNIP3, BNIP3L, LDHA and VEGFC transcripts were all up-regulated by 1% O_2/16h exposure in Hep3B treated with scrambled RNA. The 4-5-fold hypoxic induction of the BNIP3 and BNIP3L mRNA levels was entirely (BNIP3) or almost entirely (BNIP3L) driven by HIF-1α (see siHIF-1α data). Silencing USF1 and USF2a expression, however, resulted in moderately (siUSF1) or significantly (siUSF2a) increased fold hypoxic inductions of BNIP3 and BNIP3L genes. The stronger effect on the hypoxic induction of BNIP3 and BNIP3L genes by the siUSF2a treatment could result from its effective double knockdown of USF1 and USF2a proteins (Fig. 2). Elevated gene activity of LDHA in hypoxic Hep3B was weakly attenuated following siHIF-1α treatment but not impacted by either USF knockdown. Expression of 4EBP1, mildly suppressed in hypoxic hepatoma cells (scr data), was constitutively reduced upon the knockdown of USF factors. The ~2-fold hypoxic induction of VEGFC mRNA (scr data) was lost upon USF siRNA treatment due to a strong increase of transcript level in normoxic Hep3B cells.

With regard to the vividly O_2 responsive BNIP3 and BNIP3L genes, we also noted that the potentiation of the induction in USF-silenced cells subjected to 1% O_2 predominantly derived from a reduced normoxic, rather than strengthened hypoxic, gene activation (Fig. 3). This observation highlighted the importance of USF1/2a in maintaining the basal transcription of either gene in oxygenated cells. Because HIF-1 is

known to regulate BNIP3 activity with an unusually broad O_2 response profile (15, 17), the factor could likely encounter USFs at the BNIP3 promoter even in sub-normoxic cells. In additional qPCR analyses we therefore assessed if, during episodes of moderate (3% O_2) or very mild degrees of O_2 scarcity (10% O_2), HIF-1 continues to control BNIP3. We also asked if, relative to harsher hypoxia (1% O_2), USFs will compete more potently with HIF-1 for the BNIP3 regulatory binding sites at 3% and 10% O_2 (see discussion for further reasoning). Steady state levels of BNIP3 mRNA indeed revealed for scr-transfected Hep3B cells robust inductions of 3.3- and 1.6-fold in cells subjected to 16h of 3% and 10% O_2, respectively (**Table 3**). Together with the profiling at 1% O_2 (4.8-fold transcript induction), the exquisite sensitivity of the BNIP3 gene across a wide range of changes in oxygen concentrations became fully evident. Moreover, as silencing of HIF-1α expression abrogated the inductions at 1%, 3% and 10% O_2 all equally efficient down to transcript parity (i.e. H/N ratios = 1.0 for siHIF-1α treatment; see Fig. 3 and Table 3), responses of BNIP3 to 1-10% O_2 appear to rest entirely on functional HIF-1. Upon silencing of USF1, but surprisingly not USF2a, we observed the BNIP3 induction to be potentiated almost significantly at 3% O_2 {3.3-fold (scr) → 4.6-fold (siUSF1); $p = 0.070$}, and to a significant extent at 10% O_2 {1.6-fold (scr) → 2.2-fold (siUSF1); $p = 0.019$} (Table 3). This USF1 loss-of-function mediated enhancement resulted from the combination of reduced normoxic {1.0 (scr) → 0.7 (siUSF1)} and, towards milder hypoxia, progressively increasing hypoxic levels of BNIP3 transcripts {with 100% mRNA level (scr) → 84% - 95% - 105% mRNA level at 1% O_2 - 3% O_2 - 10% O_2 (siUSF1)}.

While we were encouraged by these early data suggesting a competitive crosstalk to occur between basally active HIF-1 and USF factors in cells facing a sub-normoxic milieu, the remainder of the study focused on providing proof-of-principle evidence for USF-mediated positive or negative functional interactions with HIF-1 at 1% O_2. At this level of deoxygenation HIF-1 activity peaks in many cell lines, hence, its transcriptional control of the bulk of downstream targets is expected to operate with optimal efficacy. Alignments of the homologous regions of BNIP3 promoters had revealed a remarkable hmr

conservation around the HRE motif (Suppl. Fig. S2). For this reason we went on to compare the promoter responses of BNIP3, where the HRE and CACGTG motifs are contained within a single *cis*-element, with those of MC1R, 4EBP1 and LDHA genes, which all possess distinct HRE and palindrome sites of variable hmr conservation (Table 2; Fig. S2**)**. Parallel chromatin immuno-precipitation (ChIP) experiments confirmed the recruitment of hypoxia-inducible HIF-1α- and constitutive USF1- and USF2a-containing complexes to both LDHA (**Fig. 4A**) and BNIP3 (Fig. 4B) promoter sequences in intact Hep3B (Fig. 4, left panels), MCF7 (Fig. 4, right panels) and HeLa cells (not shown). This coordinate binding of HIF-1 and USFs was seen both at low oxygen (at LDHA + BNIP3 promoter) and in oxygenated nuclei as well (see HIF-1α at BNIP3 promoter; Fig. 4). The latter finding added weight to the notion of HIF-1 controlling BNIP3 transcription even under sub-normoxic/normoxic conditions (see previous paragraph).

To further study the convergence of HIF and USF pathways at DNA level, the promoter regions in question were amplified from genomic DNA, cloned, sequence confirmed and inserted into pGL3 basic luciferase reporter plasmids. The set of luciferase promoter reporters thus obtained included both donated (i.e. BNIP3 and PHD2) and self-generated constructs (TYR, 4EBP1, LDHA, MC1R), and covered USF-specific (i.e. TYR; (43) or HIF-1 specific targets (i.e. PHD2; (44) plus four HRE/palindrome candidates (4EBP1, LDHA, MC1R, BNIP3; Table 2, Fig. S2). We initially examined the hypoxia (1% O_2/16h) responsiveness of these candidate promoters. Respective reporter transfections of Hep3B, MCF7 and HeLa cells included negative control reactions (i.e. "bVec" = empty pGL3 basic luciferase vector; **Fig. 5**) to monitor basal and hypoxia-nonresponsive LUC activity. In contrast, the PHD2 luciferase construct was induced approximately 3-8-fold in hypoxic Hep3B, HeLa and MCF7 cells **(Fig. 5)**. Luciferase assays with the four candidates 4EBP1, LDHA, MC1R and BNIP3 revealed only for LDHA (~2-fold) and BNIP3 (4-7-fold) a robust up-regulation by hypoxic conditions in Hep3B, MCF7 and HeLa cells.

Next, we investigated the possible co-regulation of BNIP3 and LDHA reporter by HIF and USF cascades in co-transfections with HIF-1α and USF1, 2a or 2b expression plasmids (**Fig. 6)**. In pilot studies (not shown), we had carefully titrated for each cell line the amount of HIF-1α plasmid (i.e. 15-100 ng) needed for an optimal hypoxic induction of either reporter and of any USF plasmid (i.e. 15 ng) needed for an optimal specific activation of either reporter construct (Fig. 6). The activity of the TYR promoter reporter rose constitutively 4-7-fold upon USF1-, and up to 20-fold upon USF2a, co-transfection. Over-expression of HIF-1α did not impact the TYR reporter (Fig. 6A). On the other hand, PHD2 reporter activity was significantly increased in normoxic and hypoxic Hep3B upon HIF-1α over-expression. The impact of over-expressed USFs on the PHD2 reporter was either negligible (USF1) or attributed to non-specific stimulation by the over-expressed factor (USF2a) exerted on the vector backbone. Therefore, both control reporters responded specifically to the over-expression of their respective transcriptional driver(s) (Fig. 6A).

The LDHA promoter was induced by endogenous hypoxia signals almost 2-fold in Hep3B (Fig. 6B), and additionally stimulated upon co-transfection with USF1, and particularly, USF2a and 2b plasmids. Of note, over-expressed USFs augmented LDHA luciferase activity predominantly under normoxia, thereby reducing the original hypoxic induction to an almost constitutive expression in Hep3B (Fig. 6B) and MCF7 cells (not shown). The switching from HIF- to USF-driven trans-activation modes, and *vice versa*, was further observed for the endogenous LDHA promoter, particularly in Hep3B (Fig. 4A, left panel) and HeLa cells (not shown). Here, hypoxia clearly promoted HIF-1 binding and, in parallel, attenuated the occupancy of USF1 and USF2a. Thus, HIF-1 and USF complexes recruited to the LDHA promoter cap the activity of one another to yield a pO_2-dependent complementation mode of gene control.

Based on these data, transactivation of the LDHA gene by HIF-1 and USFs proceeds from distinct motifs (below) and peaks at varying pO_2 (USFs → aerobic LDHA expression; HIF-1 → hypoxic LDHA expression). In contrast, both pathways must converge onto a single stretch of DNA within the BNIP3

promoter (Suppl. Fig. S2, and below). The relevant reporter was nearly 3-fold hypoxia induced by endogenous HIF-1-mediated (Fig. 3) signaling in Hep3B (Fig. 6C) and HeLa cells (Fig. 6D). Co-transfection with USF1 and 2a, or with USF2b, enhanced BNIP3 promoter activity in both cell lines particularly under normoxia and consequently weakened the reporters' hypoxic induction. Over-expression of HIF-1α amplified the hypoxic BNIP3 activity robustly in Hep3B (6.6 fold; Fig. 6C) and moderately in HeLa cells (3.2 fold, Fig. 6D). However, this potentiated hypoxia response of BNIP3 by ectopic HIF-1α was significantly impaired through the simultaneous co-transfection with USF1 or USF2a, but not USF2b, in Hep3B and HeLa cells (Figs. 6C+D: see ↓ arrows). Increasing the amount of USF1/2a plasmids further (15→100ng) converted the hypoxic trans-activation of the reporter into an increasingly constitutive response, especially in Hep3B cells (Fig. 6C). These data suggest that HIF-1α and USF1 or USF2a compete dose-dependently with each other over the control of the BNIP3 site.

The functionality of the computed HIF-1 and USF1/2 sites in the LDHA and BNIP3 promoter was assessed by EMSA screens with Hep3B, HeLa and MCF7 normoxic and hypoxic nuclear extracts. Representative results are shown for LDHA (MCF7 nuclear extracts, **Fig. 7A)** and BNIP3 (Hep3B nuclear extracts, Fig. 7B**)**. The wildtype CACGTG-motif in region I (Fig. S2) of the LDHA promoter was weakly bound by a hypoxia-regulated complex containing HIF-1α (see supershift (ss) – lane 4; Fig. 7A) and avidly bound by the constitutive complex (cc) factors USF1 and USF2a (see ss in lanes 6, 7 and 9, 10; Fig. 7A – reg.I wt). Another radiolabeled oligonucleotide, spanning the wildtype region II and III (Fig. S2: reg.II/III ww) was tightly bound both by HIF-1α and USF1/2 (Fig. 7A, lower panel; detection of HIF-1α ss: lane 4; USF2 ss: 9+10). When using a reg.II/III double site oligonucleotide carrying a mutation in region II and an unaltered wildtype sequence in region III (reg.II/III mw), only the hypoxia inducible complex, supershifted by anti-HIF-1α, was detected in conjunction with a complete loss of the constitutive binding activity by USFs (Fig. 7A: reg. II/III mw). The reverse sequence alteration in region III but not II (reg. II/III wm) left the oligonucleotide attachment by the constitutive USF complex

undisturbed, but erased any interaction with HIF-1. Thus, the LDHA-region II acts as exclusive, high-affinity site for USFs, while LDHA-region III attracts HIF-1 to this promoter in deoxygenated nuclei.

In contrast to this segregated binding of HIF-1 and USFs in the LDHA promoter, either complex interacted with the -259/-236 DNA of the BNIP3 promoter containing the HRE at -251/-246 (Fig. S2) **(**Fig. 7B**)**. Specific supershifts were able to positively identify HIF-1α (ss: lane 4) as constituent of a hypoxic binding activity (lane 2), and USF1 (ss: lanes 6+7) and USF2 (ss: lanes 9+10) as participants of a constitutive complex (cc; lanes 1+2) **(**Fig. 7B**)**. We further elaborated whether the HIF-USF interplay at the -251/-246 core element of BNIP3 is governed by differential affinities of the respective factors. To that end, we conducted additional pull-down analyses using magnetic beads coated with biotinylated wildtype (w-bio) BNIP3 HRE probes (Suppl. Table ST1) and assessed binding specificity and avidity in reactions containing 10× or 50× excess of wt competitor (comp.) oligonucleotides or beads coated with mutant (m-bio) probes (Suppl. Fig. S3). 10× and 50× excess probe diminished the initial binding activity (set to 100% in each case) to a mean (n = 3-4 independent assays) residual activity of: a) ~8.8% (10×) and ~5.4% (50×) for hypoxic HIF-1; b) ~1.3% and ~0.4% for normoxic or hypoxic USF1; and c) ~2.6% and ~1.4% for normoxic or hypoxic USF2a, respectively. The fact that 10×/50× excess probe sufficiently eliminated almost all of the USF-bead interaction demonstrated the, relative to hypoxic HIF-1, much weaker *in vitro* affinity by which USF1 and 2a constitutively bind to the BNIP3 HRE (Suppl. Fig. S3).

Discussion

One way to fine-tune, or inhibit, HIF's transcriptional outflow independently of hydroxylase activities could be through competing transcription factors. We reported earlier (18) that binding of a Hep3B factor to CACGTG motifs was able to counteract the HIF-driven induction of the phb2 reporter from HREs at adjacent positions. Evidently, palindrome factors can engage in positive or negative crosstalk with nearby

HIF/HRE complexes (45-47). En route towards a more physiological understanding of hypoxic signaling, we thought to analyze gene control mechanisms not just as a function of the stability/activity of HIF-1 *per se*. Rather, the dynamical interplay between transcriptional complexes that governs the hierarchy by which HIF-1 and related factors gain access to DNA and regulate expression was considered. The current study, thus, aimed to i) identify the phb2 CACGTG-binding entity in human cancer cells and ii) investigate the factors interplay with HIF-1 in the control of selected examples of co-targeted genes.

Both, EMSA supershifts and oligonucleotide pull-down assays consistently identified USF1 and USF2a/2b as the main phb2 CACGTG-complex in nuclear extracts from Hep3B and HeLa (Fig. 1) or MCF7 cell lines. Our pull-down assays also documented the preferential *in vitro* docking of HIF-1 to the asymmetric -107 phb2 HRE and of USFs to the symmetrical -146 phb2 palindrome motif (Fig. S1B+C, 50× comp. lanes). Thus, the single base substitution within the hexameric core of either motif (i.e. -107 HRE: 5'-TACGTG-3'; -146 palindrome: 5'-CACGTG-3'), and presumably additional changes in neighbouring nucleotides, are key in conferring the vastly differing affinities of HIF and USF transcription factors to these motifs. This observation fits well with the general perception that CACGTG-palindromes tend to attract non-HIF bHLH factors (25, 36, 37, 47), and, consequentially, are notably underrepresented amongst *functional* HIF elements (48-50). Our co-immunoprecipitations further demonstrated the interactive precipitation of HIF-1α by ARNT proteins and *vice versa* but failed to reveal any physical contact between USF2a and either subunit of HIF-1 (HIF-1α, ARNT) (see Fig. S1D+E and (41)). Thus, the constitutive USF1/2a are the main factors that indirectly interfere with the HIF/HRE-driven induction of hb2 globin gene by binding to the phb2 CACGTG palindrome in human cancer cells (18, 31).

Upstream stimulatory factors belong to the basic helix-loop-helix-leucine zipper (bHLH/ZIP) family of transcription factors (21, 51, 52). They can mutually influence each other's expression, both in positive (USF2 trans-activates USF1 gene, (42); USF2a knockdown yields diminished USF1 levels; Fig. 2) and

negative ways (USF1 represses USF2 gene; USF1$^{-/-}$ mice show elevated USF2 levels, (42)). USFs have been implicated in conferring the UV-induced tanning response in melanocytes and in acting as anti-proliferative agents in cells transformed by over-expressed MYC or activated RAS-signaling (53). Following a marked depletion of intracellular calcium during the differentiation of erythroid progenitor and erythroleukemia cells, endogenous USFs start to accumulate and trans-activate several adult marker genes (e.g. β globin) that ultimately drive the cells into maturity (54). Beyond MYC, palindrome complexes can also counteract, or interfere with, HIF's transcriptional read-out. To date, three human genes have been examined as HIF/USF co-regulated targets, i.e. the genes encoding plasminogen activator inhibitor-1 (PAI-1) (55-57), the catalytic subunit of the telomerase, the telomerase reverse transcriptase (TERT) (58-60) and the glycolytic enzyme L-type pyruvate kinase (L-PK) (41).

Guided by *Daphnia's* phb2 coordinates we conducted a genome-wide computational survey for HIF/USF-co-responsive *human* genes that were flanked by closely adjacent or over-lapping CACGTG palindrome and HRE motifs. Among those we found LDHA and BNIP3 to be expressed and hypoxia-induced at transcript level in human Hep3B cells (Fig. 3). This induction was entirely dependent (BNIP3), or aided (LDHA), by HIF-1α in Hep3B cells. The O_2-responsive control of BNIP3 via HIF-1α ranged, in Hep3Bs` at least, from harsh (1% O_2) to moderate (3% O_2) to mild (10% O_2) degrees of deoxygenation. Since the promoter of either gene recruited both HIF-1 and USFs in hypoxic Hep3B and MCF7 cells *in vivo* (Fig. 4), control of LDHA and BNIP3 expression was considered suitable to examine HIF/USF crosstalk at DNA level in greater detail. Previous studies had already validated human LDHA and BNIP3 genes as hypoxia-inducible HIF-1 targets in HeLa and MCF7, respectively (48, 61).

Luciferase reporter of the LDHA (~2-fold) and BNIP3 (3.5-7-fold) promoter yielded a robust up-regulation by hypoxic (1% O_2/16h) conditions across Hep3B, HeLa and MCF7 cells (Fig. 5). In co-transfection assays in Hep3B cells, over-expressed USFs were found to up-regulate the LDHA reporter

particularly in normoxic conditions (Fig. 6B). The role of USFs' in transactivating LDHA in oxygenated cells implies the factors as candidate drivers of aerobic glycolysis in cancer cells (Warburg effect). A previous study had already described rat LDHA as MYC target and further noticed the weak up-regulation of the gene by USFs under normoxia via binding of both E-box sites, reg. I and reg. II, within the rat LDHA promoter (62). The *human* LDHA promoter was, during low pO_2, predominantly bound by HIF-1, which, in Hep3B and HeLa but not MCF7 cells, evidently served to displace LDHA-attached USFs (Fig. 4A). Subsequent EMSA gel supershift assays revealed region I of the 5' flank of the LDHA gene as weak HIF-1 and strong USF1/2a site. The region II palindrome and region III asymmetric E-box of LDHA, however, functioned as USF1/2 (reg. II) and HIF-1 (reg. III) binding sites, respectively (Fig. 7A**)**. To rationalize these data we surmise that, in Hep3B and HeLa cells at least, the sites in regions I-III do not appear to be segregated. Upon changes in pO_2 they rather act as adaptable platform for the dominant transcription factor entity. Thus, in hypoxic Hep3Bs` and HeLas`, HIF-1 might variably expand its LDHA occupancy from its holdout at region III onto regions I and II as well and, by doing so, displaces bound USFs from these regions in intact cells. At the same time, the presence of distinct, non-overlapping sites in the LDHA promoter forms the very foundation for the complementing control of this gene by HIF-1 and USF pathways **(**Fig. 6 and 7A**)**. This complementation allows the HIF-driven expression of LDHA during hypoxia to eventually switch to a USF (and MYC)-mediated control under high pO_2 which, in turn, ensures production of this glycolytic enzyme in response to a broader O_2 spectrum and additional micro-environmental stimuli of solid malignancies (i.e. acidic milieu).

Co-transfection of Hep3B and HeLa cells with HIF-1, USF1 and 2a revealed the dose-dependent interference with the HIF-1-mediated BNIP3 induction at 1% O_2 by USFs (see ↓ arrows, Fig. 6C and D). Conversely, the transient loss of USF1+USF2a functions (siUSF2a treatment, Fig. 2), or of USF1 activity alone (siUSF1 treatment), resulted in Hep3B cells in a significantly augmented induction of BNIP3 (and BNIP3L) genes at harsh (1% O_2) and mild (10% O_2) degrees of deoxygenation, respectively **(**Fig. 3; Table 3). These data support the notion of an increasing competition of HIF`s BNIP3 control by endogenous

USF1 in mildly O_2-deprived cells (see also below). The HRE at position -251/-246 in the promoter of human BNIP3 gene was first identified by Kothari and co-workers to function as a direct functional binding site for HIF-1 under hypoxia (61). Our EMSA screen with a single site oligonucleotide (-259/-236; Suppl. Table ST1) characterized this HRE-containing sequence as being co-targeted by HIF-1 and USFs in hypoxic (1% O_2/16h) cells (Fig. 7B). Additional pull-down assays revealed hypoxic (1% O_2/16h) HIF-1 complexes to dock, *in vitro*, much more tightly to the BNIP3 HRE than do USF1 and 2a factors (Suppl. Fig. S3). Since pull-downs utilize, EMSA-like, nuclear extracts with free, DNA-dissociated alpha subunits, they cannot provide insights on the binding of normoxic HIF-1 to the *cis*-element in question. Nonetheless, we extrapolate a markedly inferior affinity of USFs to the BNIP3 HRE when compared to *hypoxic* HIF-1 complexes under *in vivo* conditions as well.

Although USF expression manipulations affected BNIP3 gene/reporter activity particularly in normoxia (i.e. note BNIP3 inductions at 1% O_2 in a) Fig. 3, USF1/2a knockdown (kd): 4.8fold (scr) → 6.6-7.6fold (kd); b) Figs. 6c, 6d; USF1/2a overexpression: 2.8fold (endogenous) → 1.5-1.8fold (overexpression)), several additional observations implied the USF/HIF convergence onto BNIP3 to follow far more intricate rules than a LDHA-like segregation between normoxic/USF and hypoxic/HIF occupations would suggest. Firstly, ChIP analysis of all three cell lines (Hep3B, MCF7, HeLa) showed measurable amounts of HIF-1 during normoxia, and of USF1/2 complexes during normoxia and hypoxia, attached to the BNIP3 promoter chromatin (Fig. 4 and data not shown). Secondly, the USF1/2 dimers, tethered to the same -251/-246 core sequence as the hypoxia-inducible factor during low pO_2 (Fig. 7B), showed virtually no signs of displacement by incoming HIF-1 (Fig. 4). Such a persisting attachment of USF factors during hypoxic periods of HIF-1 occupancy could be achieved by the presence of secondary docking sites within the BNIP3 promoter. Indeed we noted hmr conserved CACGCR motifs dubbed E1 and E2, separated by 3-nucleotide spacers on either side of the -251/-246 BNIP3 HRE (i.e. 5′ CACGCGccg**CACGTG**cca CACGCA 3′; E1/E2 = capital; spacers = small; HRE = capital/bold; see Table 2; Suppl. Fig. S2). Subsequent EMSA experiments using triple site E1-HRE-E2 oligonucleotide probes in www (all three

sites intact) and mwm (HRE intact, E1+E2 mutated) configuration revealed for hypoxic extracts (HIF-1 docked to HRE) a 1.3-2.3 fold stronger binding of USF complexes to www than mwm sequences (not shown). Thus, intact E1/E2 motifs (and several other CACGCN promoter sites) can temporarily provide alternative USFs sites at the BNIP3 gene. When HIF-1 approaches the BNIP3 HRE during low pO_2 *in vivo*, USFs may be able to sidestep displacement by sliding onto E1 and E2.

The fact that we detected HIF-1α tethered to the BNIP3 promoter in normoxia only *in vivo* (ChIP), but not by *in vitro* (EMSA, pull-down) measures, may highlight the protective effect of chromatin and/or the required HIF-1 heterodimer under conditions where free alpha subunits are all but depleted due to ongoing hydroxylation and degradation. Since none of the usual pro-inflammatory agents (e.g. cytokines, growth factors, reactive oxygen species), known to spark a strong non-hypoxic HIF-1α accumulation and induced expression of HIF-1 targets, were added to our cultures the select interaction of HIF-1 with the BNIP3 promoter in oxic cells appears to occur independently of changes in cytokine/growth factor/ROS concentrations. Regarding the question whether DNA-bound HIF-1 in oxic cells maintains transcriptional functionality, we found that, in Hep3B cells subjected to 16h periods of 3% and 10% O_2, HIF-1α still manages to drive the induction of BNIP3 (Table 3). Overall, however, our knowledge is meager at best when it comes to events emanating from HIF-signaling in mildly deoxygenated or completely aerobic cells. A noted exception is a study by Welford and colleagues which documented HIF-1 to be strictly necessary in delaying the onset of cellular senescence in aerobic murine embryonic fibroblasts, in part via the transcriptional control of the pro-inflammatory macrophage migration inhibitory factor (MIF) (63).

Taken together, the distinct sites of the LDHA promoter allow switching between USF/normoxic and HIF-1/hypoxic states, in favor of a complementing expression profile with a broadened O_2 sensitivity. In contrast, the single BNIP3 sequence around the -251/-246 CACGTG motif seems to be the platform for a

pO_2-dependent, conditional competition between USF1/2a and HIF-1 (i.e. a) normoxic/sub-normoxic state: USF↔HIF-1; b) hypoxic (1% O_2) state: HIF-1 only; with ↔ = competition). If so, this conditional competition would argue for different DNA-affinities and/or transactivation competences of normoxic and hypoxic HIF-1 complexes, respectively. Inadequate α:β subunit-interactions, however, are unlikely to be involved in debilitating affinity or transcriptional capacity of normoxic HIFs (relative to species at 1% O_2). Recent fluorescence resonance energy transfer measurements revealed, at least for proteolysis-saturating levels of over-expressed HIF-2α and ARNT, identical α:β distances in normoxic and hypoxic HIF-2 heterodimers (64). While the assembly of HIF in oxygenated and severely hypoxic nuclei appears to match one another, the α-subunits in such high-pO_2, HRE-tethered dimers should show hydroxylation at ODD-prolyl and/or CAD-asparaginyl residues.

The recent categorization of HIF-1 targets into PHD- (driven by HIF-1α NAD activity) and PHD/FIH-dependent cohorts (driven by HIF-1α NAD + CAD activity) has yielded some surprising new insights regarding the O_2-profiles of LDHA and BNIP3 genes (15-17). Here, BNIP3 expression was characterized by extremely low FIH-1 sensitivity scores, indicating full responsiveness of the gene by marginal drops of pO_2 and transcriptional gene induction (rather than inhibition) by active FIH-1. In line with this concept, we find BNIP3 to be induced via HIF-1α in hepatoma cells at 1%, 3% and 10% O_2 (Fig. 3, Table 3). While possible functions of BNIP3, in addition to the factors pro-apoptotic/pro-autophagic dichotomy (65, 66), need to be clarified for mildly versus profoundly hypoxic cancer cells, the binding of HIF-1 to the BNIP3 promoter under a wide range of pO_2, and to the LDHA sites selectively during hypoxia, agrees with such non-redundant impacts of PHDs and FIH-1 on the activity of these HIF targets. In USF-1 silenced Hep3B, BNIP3 mRNA expression levels were, relative to controls transfected with scrambled RNA, reduced in normoxic cells and steadily increasing in cells experiencing ever milder degrees of hypoxia. This mix of effects yielded, as result of the USF1 knockdown, a progressive potentiation of the BNIP3 induction from harsh (1% O_2) to moderately (3% O_2) to mildly (10% O_2) deoxygenated Hep3Bs

(Fig. 3, Table 3). We therefore surmise that *endogenous* USFs primarily cap the activity of the HIF-1/HRE complex at BNIP3 during normoxia-mild hypoxia; i.e. interfere with HIF-1 complexes whose alpha subunits remain either fully (i.e. at ODD/NAD + CAD) or partially (i.e. at CAD) hydroxylated. The HIF-1/HRE complex under strictly hypoxic (1% O_2) conditions, i.e. with complete dehydroxylation of alpha subunits at NAD and CAD regions, is, however, due to HIF´s superior DNA affinity dominant over endogenous USFs. Now, upstream stimulatory factors will only through over-expression still be able to shift the binding equilibrium to the BNIP3 HRE in their favor and guard the site against HIF-1. Thus, USF1 and 2a are best viewed as pO_2-dependent conditional, not compulsory, HIF-interfering factors. Their delimiting impact on hypoxic signaling likely occurs most effectively towards HIF's temporal or O_2-limits (i.e. during anoxia or re-oxygenation), or in response to a strong physiological activation of the USF pathway (i.e. i) UV-induced USF1 phosphorylation in cells of melanocytic origin (53); ii) Ca^{2+}-depletion based protection from proteolysis in differentiating erythroid progenitor/erythroleukemia cells (54)). Future work should tap into genome-wide implications of co-activated cross talk between endogenous USFs and HIF-1 in appropriate models.

Acknowledgements:

We are grateful to Dr. Benoit Viollet (Institut Cochin INSERM, Universite Paris, Paris France) for his generous gifts of USF antibodies and expression plasmids and his unwavering willingness to act as expert sounding board throughout the project. We also thank the following colleagues for their kind contributions of various materials: Prof. Adrian L. Harris (John Radcliffe Hospital, Oxford, UK); Dr. Makoto Tsuneoka (Kurume University, Fukuoka, Japan); Prof. Richard S. Pollenz (University of South Florida, Tampa); Prof. Kazuhiro Sogawa (Tonoku University, Sendai, Japan); Prof. Robert G. Roeder (Rockefeller University, New York, USA); Prof. P. Maxwell (University College London, London, UK) and Prof. J. Okami (University of Michigan). We thank Ms. Kristin Wollenick (Institute of Physiology, University of Zurich) for the short version of PHD2 luciferase reporter plasmid and Mr. Kristian Reveles Jensen for his help as a BUSS-2008 summer student at the University of Zurich. Lastly, the authors would like to thank two anonymous reviewers whose helpful and constructive comments aided greatly in improving the manuscripts` discussion. This work was made possible by grants from the EU's 6th framework programme (Euroxy consortium; partners: MG, TAG) and the Swiss National Science Foundation (MG).

References

1. Centanin L, Gorr TA, Wappner P. Tracheal remodelling in response to hypoxia. J Insect Physiol. 2010;56:447-54.
2. Gorr TA, Gassmann M, Wappner P. Sensing and responding to hypoxia via HIF in model invertebrates. J Insect Physiol. 2006;52:349-64.
3. Fandrey J, Gorr TA, Gassmann M. Regulating cellular oxygen sensing by hydroxylation. Cardiovasc Res. 2006;71:642-51.
4. Wang GL, Jiang BH, Rue EA, Semenza GL. Hypoxia-inducible factor 1 is a basic-helix-loop-helix-PAS heterodimer regulated by cellular O2 tension. Proc Natl Acad Sci U S A. 1995;92:5510-4.
5. Epstein AC, Gleadle JM, McNeill LA, Hewitson KS, O'Rourke J, Mole DR, et al. C. elegans EGL-9 and mammalian homologs define a family of dioxygenases that regulate HIF by prolyl hydroxylation. Cell. 2001;107:43-54.
6. Ivan M, Kondo K, Yang H, Kim W, Valiando J, Ohh M, et al. HIFalpha targeted for VHL-mediated destruction by proline hydroxylation: implications for O2 sensing. Science. 2001;292:464-8.
7. Jaakkola P, Mole DR, Tian YM, Wilson MI, Gielbert J, Gaskell SJ, et al. Targeting of HIF-alpha to the von Hippel-Lindau ubiquitylation complex by O2-regulated prolyl hydroxylation. Science. 2001;292:468-72.
8. Krek W. VHL takes HIF's breath away. Nat Cell Biol. 2000;2:E121-3.
9. Lando D, Peet DJ, Gorman JJ, Whelan DA, Whitelaw ML, Bruick RK. FIH-1 is an asparaginyl hydroxylase enzyme that regulates the transcriptional activity of hypoxia-inducible factor. Genes Dev. 2002;16:1466-71.
10. Lando D, Peet DJ, Whelan DA, Gorman JJ, Whitelaw ML. Asparagine hydroxylation of the HIF transactivation domain a hypoxic switch. Science. 2002;295:858-61.
11. Wenger RH, Stiehl DP, Camenisch G. Integration of oxygen signaling at the consensus HRE. Sci STKE. 2005;2005:re12.
12. Manalo DJ, Rowan A, Lavoie T, Natarajan L, Kelly BD, Ye SQ, et al. Transcriptional regulation of vascular endothelial cell responses to hypoxia by HIF-1. Blood. 2005;105:659-69.
13. Koivunen P, Hirsilä M, Günzler V, Kivirikko KI, Myllyharju J. Catalytic Properties of the Asparaginyl Hydroxylase (FIH) in the Oxygen Sensing Pathway Are Distinct from Those of Its Prolyl 4-Hydroxylases. J Biol Chem. 2004;279:9899-904.
14. Stolze IP, Tian YM, Appelhoff RJ, Turley H, Wykoff CC, Gleadle JM, et al. Genetic analysis of the role of the asparaginyl hydroxylase factor inhibiting hypoxia-inducible factor (FIH) in regulating hypoxia-inducible factor (HIF) transcriptional target genes [corrected]. J Biol Chem. 2004;279:42719-25.
15. Dayan F, Roux D, Brahimi-Horn MC, Pouysségur J, Mazure NM. The oxygen sensor factor-inhibiting hypoxia-inducible factor-1 controls expression of distinct genes through the bifunctional transcriptional character of hypoxia-inducible factor-1alpha. Cancer Res. 2006;66:3688-98.
16. Dayan F, Monticelli M, Pouysségur J, Pecou E. Gene regulation in response to graded hypoxia: the non-redundant roles of the oxygen sensors PHD and FIH in the HIF pathway. J Theor Biol. 2009;259:304-16.
17. Pouysségur J, Dayan F, Mazure NM. Hypoxia signalling in cancer and approaches to enforce tumour regression. Nature. 2006;441:437-43.
18. Gorr TA, Cahn JD, Yamagata H, Bunn HF. Hypoxia-induced synthesis of hemoglobin in the crustacean Daphnia magna is hypoxia-inducible factor-dependent. J Biol Chem. 2004;279:36038-47.
19. Gorr TA, Tomita T, Wappner P, Bunn HF. Regulation of Drosophila hypoxia-inducible factor (HIF) activity in SL2 cells: identification of a hypoxia-induced variant isoform of the HIFalpha homolog gene similar. J Biol Chem. 2004;279:36048-58.
20. Gorr TA, Wichmann D, Pilarsky C, Theurillat JP, Fabrizius A, Laufs T, et al. Old proteins - new locations: myoglobin, haemoglobin, neuroglobin and cytoglobin in solid tumours and cancer cells. Acta Physiol (Oxf) 2011;202:563-581.

21. Viollet B, Lefrancois-Martinez AM, Henrion A, Kahn A, Raymondjean M, Martinez A. Immunochemical characterization and transacting properties of upstream stimulatory factor isoforms. J Biol Chem. 1996;271:1405-15.
22. Turley H, Wykoff CC, Troup S, Watson PH, Gatter KC, Harris AL. The hypoxia-regulated transcription factor DEC1 (Stra13, SHARP-2) and its expression in human tissues and tumours. J Pathol. 2004;203:808-13.
23. Tsuneoka M, Nakano F, Ohgusu H, Mekada E. c-myc activates RCC1 gene expression through E-box elements. Oncogene. 1997;14:2301-11.
24. Holmes JL, Pollenz RS. Determination of aryl hydrocarbon receptor nuclear translocator protein concentration and subcellular localization in hepatic and nonhepatic cell culture lines: development of quantitative Western blotting protocols for calculation of aryl hydrocarbon receptor and aryl hydrocarbon receptor nuclear translocator protein in total cell lysates. Mol Pharmacol. 1997;52:202-11.
25. Sogawa K, Nakano R, Kobayashi A, Kikuchi Y, Ohe N, Matsushita N, et al. Possible function of Ah receptor nuclear translocator (Arnt) homodimer in transcriptional regulation. Proc Natl Acad Sci U S A. 1995;92:1936-40.
26. Kaulen H, Pognonec P, Gregor PD, Roeder RG. The Xenopus B1 factor is closely related to the mammalian activator USF and is implicated in the developmental regulation of TFIIIA gene expression. Mol Cell Biol. 1991;11:412-24.
27. Okami J, Simeone DM, Logsdon CD. Silencing of the hypoxia-inducible cell death protein BNIP3 in pancreatic cancer. Cancer Res. 2004;64:5338-46.
28. Metzen E, Stiehl DP, Doege K, Marxsen JH, Hellwig-Burgel T, Jelkmann W. Regulation of the prolyl hydroxylase domain protein 2 (phd2/egln-1) gene: identification of a functional hypoxia-responsive element. Biochem J. 2005;387:711-7.
29. Cockman ME, Masson N, Mole DR, Jaakkola P, Chang GW, Clifford SC, et al. Hypoxia inducible factor-alpha binding and ubiquitylation by the von Hippel-Lindau tumor suppressor protein. J Biol Chem. 2000;275:25733-41.
30. North S, Espanel X, Bantignies F, Viollet B, Vallet V, Jalinot P, et al. Regulation of cdc2 gene expression by the upstream stimulatory factors (USFs). Oncogene. 1999;18:1945-55.
31. Gorr TA, Rider CV, Wang HY, Olmstead AW, LeBlanc GA. A candidate juvenoid hormone receptor cis-element in the Daphnia magna hb2 hemoglobin gene promoter. Mol Cell Endocrinol. 2006;247:91-102.
32. Gustafsson MV, Zheng X, Pereira T, Gradin K, Jin S, Lundkvist J, et al. Hypoxia requires notch signaling to maintain the undifferentiated cell state. Dev Cell. 2005;9:617-28.
33. Chen L, Shen YH, Wang X, Wang J, Gan Y, Chen N, et al. Human prolyl-4-hydroxylase alpha(I) transcription is mediated by upstream stimulatory factors. J Biol Chem. 2006;281:10849-55.
34. Esteban MA, Tran MG, Harten SK, Hill P, Castellanos MC, Chandra A, et al. Regulation of E-cadherin expression by VHL and hypoxia-inducible factor. Cancer Res. 2006;66:3567-75.
35. Holmquist-Mengelbier L, Fredlund E, Lofstedt T, Noguera R, Navarro S, Nilsson H, et al. Recruitment of HIF-1alpha and HIF-2alpha to common target genes is differentially regulated in neuroblastoma: HIF-2alpha promotes an aggressive phenotype. Cancer Cell. 2006;10:413-23.
36. Swanson HI, Chan WK, Bradfield CA. DNA binding specificities and pairing rules of the Ah receptor, ARNT, and SIM proteins. J Biol Chem. 1995;270:26292-302.
37. Swanson HI, Yang JH. Specificity of DNA binding of the c-Myc/Max and ARNT/ARNT dimers at the CACGTG recognition site. Nucleic Acids Res. 1999;27:3205-12.
38. Grandori C, Cowley SM, James LP, Eisenman RN. The Myc/Max/Mad network and the transcriptional control of cell behavior. Annu Rev Cell Dev Biol. 2000;16:653-99.
39. Grandori C, Mac J, Siebelt F, Ayer DE, Eisenman RN. Myc-Max heterodimers activate a DEAD box gene and interact with multiple E box-related sites in vivo. Embo J. 1996;15:4344-57.
40. Kvietikova I, Wenger RH, Marti HH, Gassmann M. The transcription factors ATF-1 and CREB-1 bind constitutively to the hypoxia-inducible factor-1 (HIF-1) DNA recognition site. Nucleic Acids Res. 1995;23:4542-50.

41. Krones A, Jungermann K, Kietzmann T. Cross-talk between the signals hypoxia and glucose at the glucose response element of the L-type pyruvate kinase gene. Endocrinology. 2001;142:2707-18.
42. Sirito M, Lin Q, Deng JM, Behringer RR, Sawadogo M. Overlapping roles and asymmetrical cross-regulation of the USF proteins in mice. Proc Natl Acad Sci U S A. 1998;95:3758-63.
43. Galibert MD, Carreira S, Goding CR. The Usf-1 transcription factor is a novel target for the stress-responsive p38 kinase and mediates UV-induced Tyrosinase expression. Embo J. 2001;20:5022-31.
44. Stiehl DP, Wirthner R, Koditz J, Spielmann P, Camenisch G, Wenger RH. Increased prolyl 4-hydroxylase domain proteins compensate for decreased oxygen levels. Evidence for an autoregulatory oxygen-sensing system. J Biol Chem. 2006;281:23482-91.
45. Kim JW, Gao P, Liu YC, Semenza GL, Dang CV. Hypoxia-inducible factor 1 and dysregulated c-Myc cooperatively induce vascular endothelial growth factor and metabolic switches hexokinase 2 and pyruvate dehydrogenase kinase 1. Mol Cell Biol. 2007;27:7381-93.
46. Lendahl U, Lee KL, Yang H, Poellinger L. Generating specificity and diversity in the transcriptional response to hypoxia. Nat Rev Genet. 2009;10:821-32.
47. Mazure NM, Chauvet C, Bois-Joyeux B, Bernard MA, Nacer-Cherif H, Danan JL. Repression of alpha-fetoprotein gene expression under hypoxic conditions in human hepatoma cells: characterization of a negative hypoxia response element that mediates opposite effects of hypoxia inducible factor-1 and c-Myc. Cancer Res. 2002;62:1158-65.
48. Firth JD, Ebert BL, Ratcliffe PJ. Hypoxic regulation of lactate dehydrogenase A. Interaction between hypoxia-inducible factor 1 and cAMP response elements. J Biol Chem. 1995;270:21021-7.
49. Semenza GL, Roth PH, Fang HM, Wang GL. Transcriptional regulation of genes encoding glycolytic enzymes by hypoxia-inducible factor 1. J Biol Chem. 1994;269:23757-63.
50. Wenger RH, Gassmann M. Oxygen(es) and the hypoxia-inducible factor-1. Biol Chem. 1997;378:609-16.
51. Sirito M, Lin Q, Maity T, Sawadogo M. Ubiquitous expression of the 43- and 44-kDa forms of transcription factor USF in mammalian cells. Nucleic Acids Res. 1994;22:427-33.
52. Sirito M, Walker S, Lin Q, Kozlowski MT, Klein WH, Sawadogo M. Members of the USF family of helix-loop-helix proteins bind DNA as homo- as well as heterodimers. Gene Expr. 1992;2:231-40.
53. Corre S, Galibert MD. Upstream stimulating factors: highly versatile stress-responsive transcription factors. Pigment Cell Res. 2005;18:337-48.
54. Lin IJ, Zhou Z, Crusselle-Davis VJ, Moghimi B, Gandhi K, Anantharaman A, et al. Calpeptin increases the activity of upstream stimulatory factor and induces high level globin gene expression in erythroid cells. J Biol Chem. 2009;284:20130-5.
55. Dimova EY, Kietzmann T. Cell type-dependent regulation of the hypoxia-responsive plasminogen activator inhibitor-1 gene by upstream stimulatory factor-2. J Biol Chem. 2006;281:2999-3005.
56. Fink T, Kazlauskas A, Poellinger L, Ebbesen P, Zachar V. Identification of a tightly regulated hypoxia-response element in the promoter of human plasminogen activator inhibitor-1. Blood. 2002;99:2077-83.
57. Samoylenko A, Roth U, Jungermann K, Kietzmann T. The upstream stimulatory factor-2a inhibits plasminogen activator inhibitor-1 gene expression by binding to a promoter element adjacent to the hypoxia-inducible factor-1 binding site. Blood. 2001;97:2657-66.
58. Chang JT, Yang HT, Wang TC, Cheng AJ. Upstream stimulatory factor (USF) as a transcriptional suppressor of human telomerase reverse transcriptase (hTERT) in oral cancer cells. Mol Carcinog. 2005;44:183-92.
59. Goueli BS, Janknecht R. Regulation of telomerase reverse transcriptase gene activity by upstream stimulatory factor. Oncogene. 2003;22:8042-7.
60. Yatabe N, Kyo S, Maida Y, Nishi H, Nakamura M, Kanaya T, et al. HIF-1-mediated activation of telomerase in cervical cancer cells. Oncogene. 2004;23:3708-15.

61. Kothari S, Cizeau J, McMillan-Ward E, Israels SJ, Bailes M, Ens K, et al. BNIP3 plays a role in hypoxic cell death in human epithelial cells that is inhibited by growth factors EGF and IGF. Oncogene. 2003;22:4734-44.
62. Shim H, Dolde C, Lewis BC, Wu CS, Dang G, Jungmann RA, et al. c-Myc transactivation of LDH-A: implications for tumor metabolism and growth. Proc Natl Acad Sci U S A. 1997;94:6658-63.
63. Welford SM, Bedogni B, Gradin K, Poellinger L, Broome Powell M, Giaccia AJ. HIF1alpha delays premature senescence through the activation of MIF. Genes Dev. 2006;20:3366-71.
64. Konietzny R, Konig A, Wotzlaw C, Bernadini A, Berchner-Pfannschmidt U, Fandrey J. Molecular imaging: into in vivo interaction of HIF-1alpha and HIF-2alpha with ARNT. Ann N Y Acad Sci. 2009;1177:74-81.
65. Bellot G, Garcia-Medina R, Gounon P, Chiche J, Roux D, Pouyssegur J, et al. Hypoxia-induced autophagy is mediated through hypoxia-inducible factor induction of BNIP3 and BNIP3L via their BH3 domains. Mol Cell Biol. 2009;29:2570-81.
66. Mazure NM, Pouyssegur J. Atypical BH3-domains of BNIP3 and BNIP3L lead to autophagy in hypoxia. Autophagy. 2009;5:868-9.
67. Corre S, Primot A, Sviderskaya E, Bennett DC, Vaulont S, Goding CR, et al. UV-induced expression of key component of the tanning process, the POMC and MC1R genes, is dependent on the p-38-activated upstream stimulating factor-1 (USF-1). J Biol Chem. 2004;279:51226-33.
68. Semenza GL, Jiang BH, Leung SW, Passantino R, Concordet JP, Maire P, et al. Hypoxia response elements in the aldolase A, enolase 1, and lactate dehydrogenase A gene promoters contain essential binding sites for hypoxia-inducible factor 1. J Biol Chem. 1996;271:32529-37.

Legends

Table 1. Top 10 pathways enriched with HRE/CACGTG-genes. Pathways with the most significant overrepresentation of HRE/CACGTG-genes are listed with their GeneGo Name, a brief description and a p-value indicating the significance of the overrepresentation of HRE/CACGTG-genes. The Network Objects column gives the number of network objects of the pathway encoded by HRE/CACGTG-genes over the total number of network objects in the pathway. The last column shows the gene symbols of the HRE/CACGTG-genes in the pathways. Bold Gene Symbols denote multiple HRE-CACGTG signatures flanking the gene, while Symbols in normal font contain one HRE-CACGTG signature in their promoter. A more detailed description of these HRE-CACGTG gene candidates can be found in the gene Excel list available upon request.

Table 2. E-box palindromes and HRE sites in promoters of human genes. HIF-1 and USF co-regulated candidate genes: 4EBP1, LDHA, MC1R and BNIP3; control genes: TYR and PHD2. Translation start site ATG as +1 (in brackets). 5' flanking region upstream of ATG is given for human TYR, PHD2, 4EBP1, LDHA, MC1R and BNIP3 genes. HRE and E-box palindromes are capitalized. Human-mouse-rat (hmr) conserved HREs: bold + underlined; variable HREs: bold only; hmr conserved E-boxes: italicized + underlined; variable E-box: italics only. For conservation: see alignments in Fig. S2.

Table 3. BNIP3 mRNA fold inductions in mildly deoxygenated Hep3B transfected with siRNAs. Hep3B transfections with scrambled (scr) control RNA or HIF-1α, USF1 or USF2a siRNA followed the identical protocol used for the quantitative expression analyses in Fig. 3 (see there). BNIP3 mRNA levels were quantified by real-time PCR and normalized by L28 expression. Fold inductions of BNIP3 transcript levels in mildly deoxygenated (H: 3% or 10% O_2; 16h) versus normoxic (N: air; 16h) Hep3B are given as means (± SD) of three independent experiments. P-values for H/N-fold changes between siRNA-treated

experimental groups (i.e. siX = siHIF-1α or siUSF1 or siUSF2a) and the scr control group of the same O_2 category (i.e. comparison done only within 3% or 10% O_2 category) are indicated.

Fig. 1. EMSA supershifts and pull–down analysis to identify phb2-binding CACGTG complex in Hep3B cells. (A) To identify factor(s) able to bind to the -146 CACGTG motif in phb2, we used the following antibodies in EMSA supershift reactions with Hep3B normoxic nuclear extracts as indicated in the figure underneath each lane. (-): no antibody; PI: pre-immune serum; ns: non-specific; cc: constitutive CACGTG complex; ss: supershifted CACGTG complex. From lane 4-13, EMSA reactions were supplemented by corresponding pre-immune (PI) and immune serum from the same rabbit used to generate anti-USF directed antibodies (e.g. lanes 4+5: PI-1M and anti-USF1M). Results reproduced in n = 3 independent assays. (B+C) Pull-down analysis with beads coated with -146 phb2 E-box-carrying oligonucleotides (5'-CACGTG-3') and HeLa normoxic (N) and hypoxic (H) nuclear extracts. Binding specificity was assessed either through beads coated with -146 mutant (m-bio) E-box motifs (5'-CAATGT-3') or with binding reactions containing 50-fold molar excess of free wild type oligonucleotide as competitor (50×comp.). Immunoblot of bound factors with (B) α-USF1M and (C) left panel: α-USF2G antibody; right panel: α-USF2aO antibody. Staining of non-specific (ns) proteins indicated as loading control. Results reproduced in n = 3-4 independent assays.

Fig. 2. Western blot analysis for transient siRNA knockdown efficiency for HIF-1α, USF1 and USF2a in Hep3B cells. Transfections with scrambled siRNA (scr) and non-transfected cells (non-TF) were used as negative controls. Cells were harvested at two post-siRNA transfection time points: 48h and 72h. Hypoxia (H, 1% O_2) exposure started at time point 42h post-siRNA transfection for 6h and 30h, respectively. Normoxia (N): air exposure. As shown in the figure, protein level expression of HIF-1α and each USF in transiently transfected Hep3B cells was robustly silenced from 48h (= 42h + 6h hypoxia) up to 72h (= 42h + 30h hypoxia) post-siRNA transfection.

Fig. 3. Real-time quantitative PCR for (top left – bottom right) BNIP3, BNIP3L, LDHA, 4EBP1 and VEGFC mRNA levels in Hep3B transfected with siRNAs. Hep3B cells were transfected with HIF-1α, USF1 or USF2a siRNA at a final concentration of 200nM. Scrambled siRNA (scr) was used as negative control. RNA was isolated from Hep3B at 66h post-siRNA transfection, i.e. at a time point where the silencing effect of HIF-1α and USFs was still in effect (see Fig. 2). Hypoxia (1% O_2) exposure started at time point 50h post-siRNA transfection for 16h. Normoxia (N): air exposure. mRNA levels of above named genes were quantified by real-time PCR and normalized by L28 expression. All data were presented as the means ± SD of four independent experiments. N: air; H: 1% O_2 16h. Mean H/N-fold inductions of each transcript are indicated above the respective pair of columns. Mean expression of individual transcripts were compared a) within same O_2 category (N or H), and b) for H/N-fold changes of siRNA-treated experimental groups (siHIF-1α, siUSF1, siUSF2a) relative to scr controls. For these scr/si-comparisons, the used symbol denotes pairwise non-parametric Wilcoxon rank-sum tests (#). See Materials and Methods for more details.

Fig. 4. Chromatin immunoprecipitation (ChIP) determination of *in vivo* HIF-1 and USF binding to LDHA and BNIP3 promoters. ChIP assay was performed in Hep3B (left panels) and MCF7 (right panels) cells using indicated antibodies or pre-immune serum and non-specific antibody IgG as negative controls. Purified DNA was subjected to PCR using LDHA primer (panel A: 159 bp amplicon) or BNIP3 primer (panel B: 314 bp amplicon). N: air; H: 1% O_2 4 h. PI-2G pre-immune serum for anti-USF2G; neg. PCR with H_2O.

Fig. 5. Endogenous response of PHD2, 4EBP1, LDHA, MC1R and BNIP3 luciferase reporter. Hep3B (A), MCF7 (B) and HeLa (C) cells were transfected with 2.0μg of 4EBP1, LDHA and MC1R or 1.5μg of PHD2 or BNIP3 luciferase reporter plasmid in a total of 3.0μg plasmid. After 16h hypoxic (1%

O_2) exposure (H, black bars) or normoxic (air) exposure (N, white bars), relative luciferase activity was determined and normalized with β–galactosidase activity (%RLA, as mean ± SD). Plasmid-free transfections (null) and transfections with the empty pGL3 basic vector (bVec) were used as negative controls. Mean H/N-fold inductions of each reporter are indicated above the respective pair of columns.

Fig. 6. Regulation of BNIP3 and LDHA luciferase activity by over-expressed HIF-1α and USFs. (A) Hep3B transfections of USF and HIF-1 control reporter using either 1.5μg TYR plasmid or 0.5μg PHD2 plasmid. (B) Hep3B transfections with 0.3μg LDHA reporter plasmid. (C) Hep3B or (D) HeLa transfections with 0.3μg BNIP3 reporter plasmid. For reporter regulation by over-expressed HIF-1α and USFs, ng amounts of HIF-1α and USF expression plasmids used are indicated underneath the respective co-transfection. Relative luciferase activity is given as in Fig. 5 (mean ± SD %RLA; n = 3 independent experiments). N, H conditions and presentation of mean H/N-fold inductions as in Fig. 3. Statistics done in regard to same O_2 category (i.e. N or H): a) endo/exo test = endogenous controls (reporter alone; no over-expressed HIF/USF) *versus* HIF/USF co-transfection (reporter with exogenous HIF-1α and/or USF1/2a); b) hif/combi test: reporter + exogenous HIF1α *versus* reporter + exogenous (HIF1α + USF1/2a). Symbols for $p < 0.05$ for i) non-parametric Wilcoxon rank-sum tests (endo/exo = #; hif/combi = ¶); ii) Anova/Sidak tests (endo/exo = ∗; hif/combi = +). See Material & Methods for more details.

Fig. 7. EMSA supershifts with LDHA and BNIP3 E-box oligonucleotides. Gel supershift using LDHA HRE and E-box palindrome oligonucleotides together with MCF7 nuclear extracts (panel A) and BNIP3 HRE oligonucleotides together with Hep3B nuclear extracts (panel B). All oligonucleotides used in this EMSA are listed in Table ST1. For HIF-1α or USFs gel supershifts, 1μl of the indicated specific antibody was used in comparison with pre-immune serum (PI-1M or PI-2G) or non-specific lgG as negative control. N, H, cc, ss: as above.

Table 1

GeneGo Pathway Name	**Pathway Description**	**pValue**	**Network objects**	**Enriched Network Gene symbols** (normal: single HRE-CACGTG signature; bold: multiple HRE-CACGTG signatures)
Insulin regulation of translation	Control of cap-dependent mRNA translation - from Insulin receptor (INSR) to Pi3k, Akt, mTOR + eIF4F	3.108e-6	10/42	eEF2K, eIF2B5, **eIF4E,** 4EBP1, **eIF4G1,** eIF4H, **INSR,** MAPK1, **PDPK1,** PRKCZ;
Androgen Receptor (AR) nuclear signalling	Control of cell adhesion, apoptosis and cholesterol metabolism via AR	6.079e-6	10/45	**EGFR,** IGF1R, KLK3, MAPK1, **RAD9A,** SCAP, SMAD3, **SRD5A1**, STAT3, **WNT10A;**
Role of IL-8 in angiogenesis	Control of angiogenesis + cell migration via interleukin 8 + VEGFA	1.064e-5	11/58	ACTR3B (= ARP3B), CARD11, **EGFR,** FASN, MBTPS1 (= S1P), **NFkBIE (= I-kBE), PDPK1,** RELB (NFkB), SCAP, SREBF1, STAT3;
Receptor-mediated HIF regulation	Control of HIF-1α translation in normoxia – from INSR → mTOR	1.288e-5	9/39	**eIF4E,** 4EBP1, HIF1A, IGF1R, **INSR**, IRS4, MAPK1, **PDPK1,** PRKCZ;
Cytoskeleton remodeling	Control of cell adhesion + motility - from extracellular matrix to actin filaments	3.350e-5	14/102	**ACTN2,** ACTR3B (= ARP3B), BCAR1, **CFL2, eIF4E,** 4EBP1, **eIF4G1/3 (eIF4G1, eIF4G3)**, eIF4H, **LIMK1,** MAPK1, PLAT (= tPA), **RPS6KA5 (= S6K 90kDa sub., MSK1**), SMAD3;
Ligand-independent activation of ESR1 and ESR2	Control of cellular proliferation + migration via Estrogen receptor β	3.636e-5	9/44	DRD1 (= Dopamine Receptor D1, GPCR), **EGFR,** ESR2 (= ER beta), GNAS (= Galpha-s), IGF1R, MAPK1 (ERK1, ERK2), **PDPK1,** PRKAR1B;
Role of SCF complex in cell cycle regulation	Control of cell cycle progression via protein ubiquitylation	8.933e-5	7/29	ANAPC (subunit 1/**2**/4 + FZR1), **CDK4,** CUL1/RBX1 E3 ligase (CUL1 + RBX1), E2F1, **FBXO5 (=Emi1)**, PLK1, SMAD3;
Insulin regulation of fatty acid methabolism	Control of fatty acid homeostasis via insulin/INSR and glucose	1.301e-4	12/88	FASN, **INSR,** MAPK1, MBTPS1 (= S1P), **PDE3B, PDPK1,** PRKAR1B, SCAP, **SLC2A4 (= GLUT4)**, SREBF1 (3 SREBP1 transcript variants);
Apoptosis and survival_BAD phosphorylation	Control of apoptosis and autophagy – from EGFR to mitochondria	1.685e-4	8/42	**BAX, EGFR,** GNAS (= Galpha-s), **GNB2 (= Gbeta2)**, IGF1R, MAPK1, **PDPK1,** PPM1A (=PP2C), PRKAR1B;
CREB pathway	Control of amino acid metabolism + cell cycle – from IGF1R+Ca channels → CREB1 transcription factor	2.366e-4	8/44	CaMK II (sub. delta + **gamma**), DRD1 (= Dopamine Receptor D1, GPCR), GNAS (= Ga-s), IGF1R, MAPK1, **PDPK1, PDYN,** PRKAR1B, **RPS6KA5 (= S6K 90kDa sub., MSK1)**;

Table 2

Gene	Sequence 5′-3′	Ref.
*h*TYR	-183 -178 -91 -86 gaaaagtcagt*CATGTG*cttttca---gccaaga*CATGTG*ataat---aggaaga(atg)	(67)
*h*PHD2	-413 -408 gccgtggtg**TACGTG**cagagcgcgcagagcgagt---gccgccgccgcc(atg)	(28)
*h*4EBP1	-179 -174 -120 -115 ggggatcc*CACGTG*gaagc--caaatcccagg**GGCGTG**gggcgg--gagacc(atg)	
*h*LDHA	-2465 -2460 -2367 -2362 -2353 -2348 cagcg*CACGTG*gagcg--actca*CACGTG*ggttcccg**CACGTC**cgccggc--aat(atg)	(62, 68)
*h*MC1R	-742 -737 -461 -456 acgttga*CAGCTG*agttgctg--ccccgg*CATGTG*gccgccct--ggacaggact(atg)	(67)
*h*BNIP3	-251 -246 cgcgcacgcgccg**CACGTG**ccacacgcacccca---gccctctggcgcc(atg)	(61)

Table 3

	scr	siHIF-1α	siUSF1	siUSF2a
O_2				
3% p (siX - vs scr)	**3.325** ± 0.754 -	**1.078** ± 0.148 p = 0.0072	**4.583** ± 0.472 p = 0.0704	**4.222** ± 0.907 ns
10% p (siX - vs scr)	**1.622** ± 0.177 -	**1.055** ± 0.038 p = 0.0056	**2.145** ± 0.159 p = 0.0189	**1.560** ± 0.313 ns

Hu et al. Figure 1

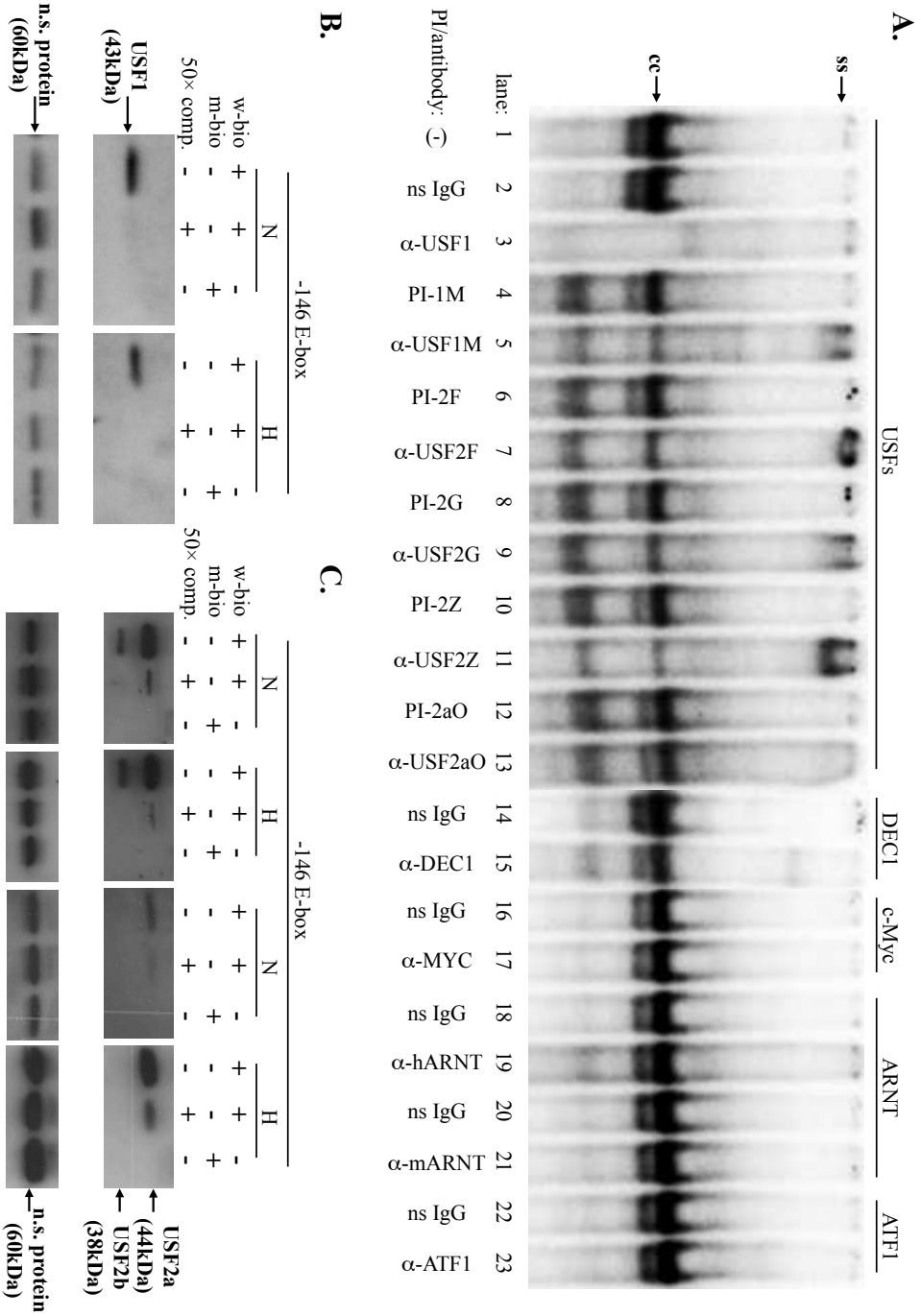

Hu et al. Figure 2

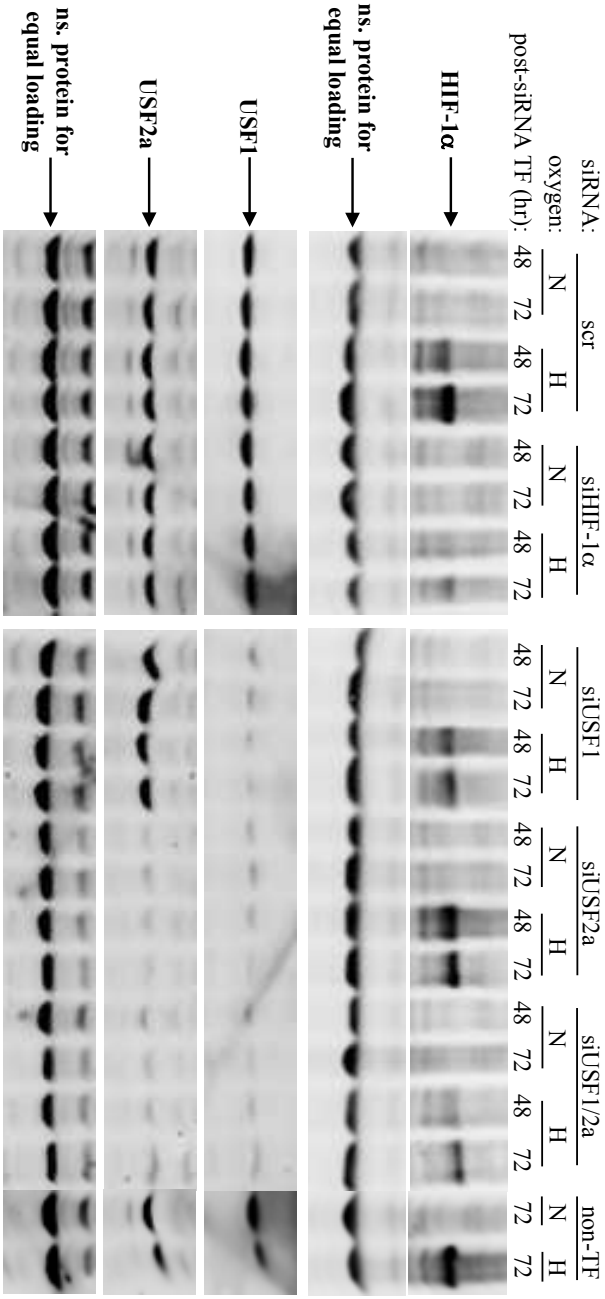

Hu et al. Figure 3

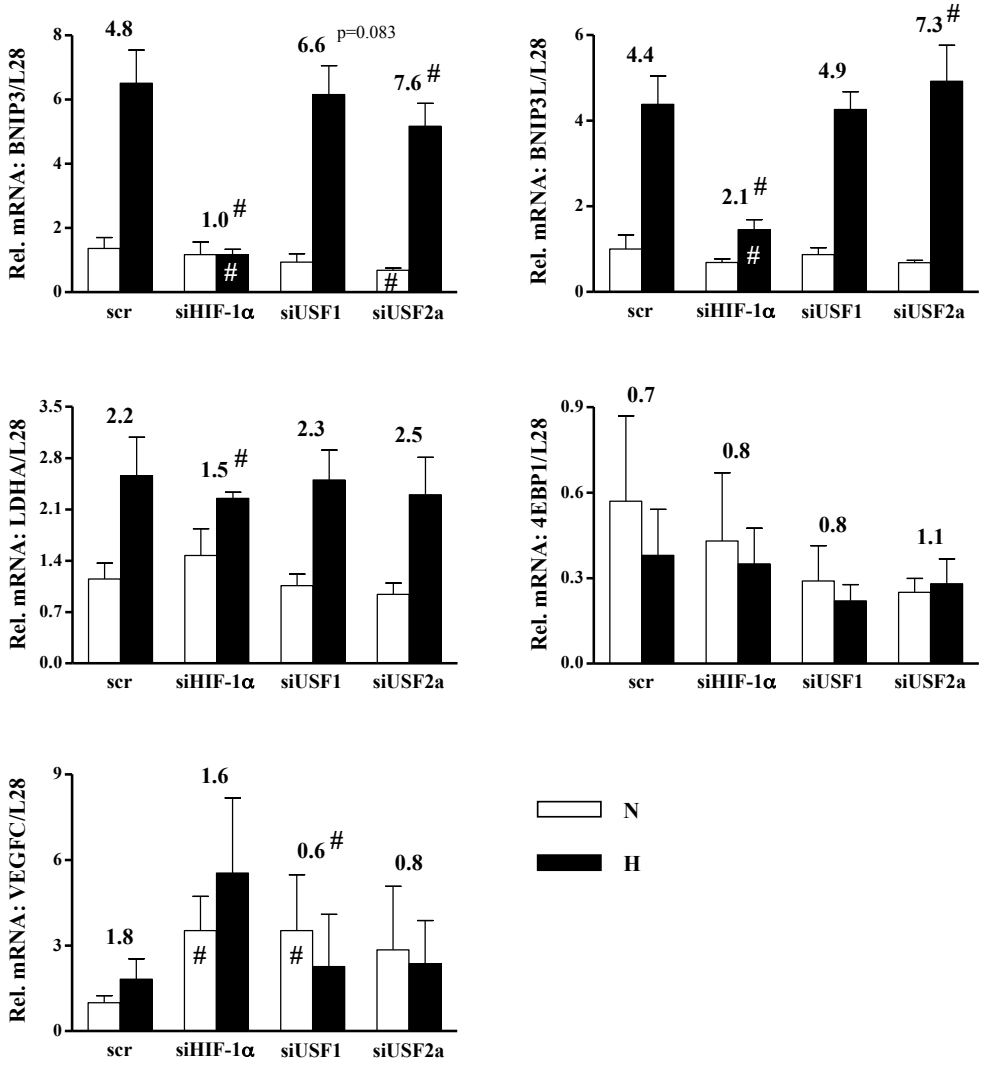

Hu et al. Figure 4

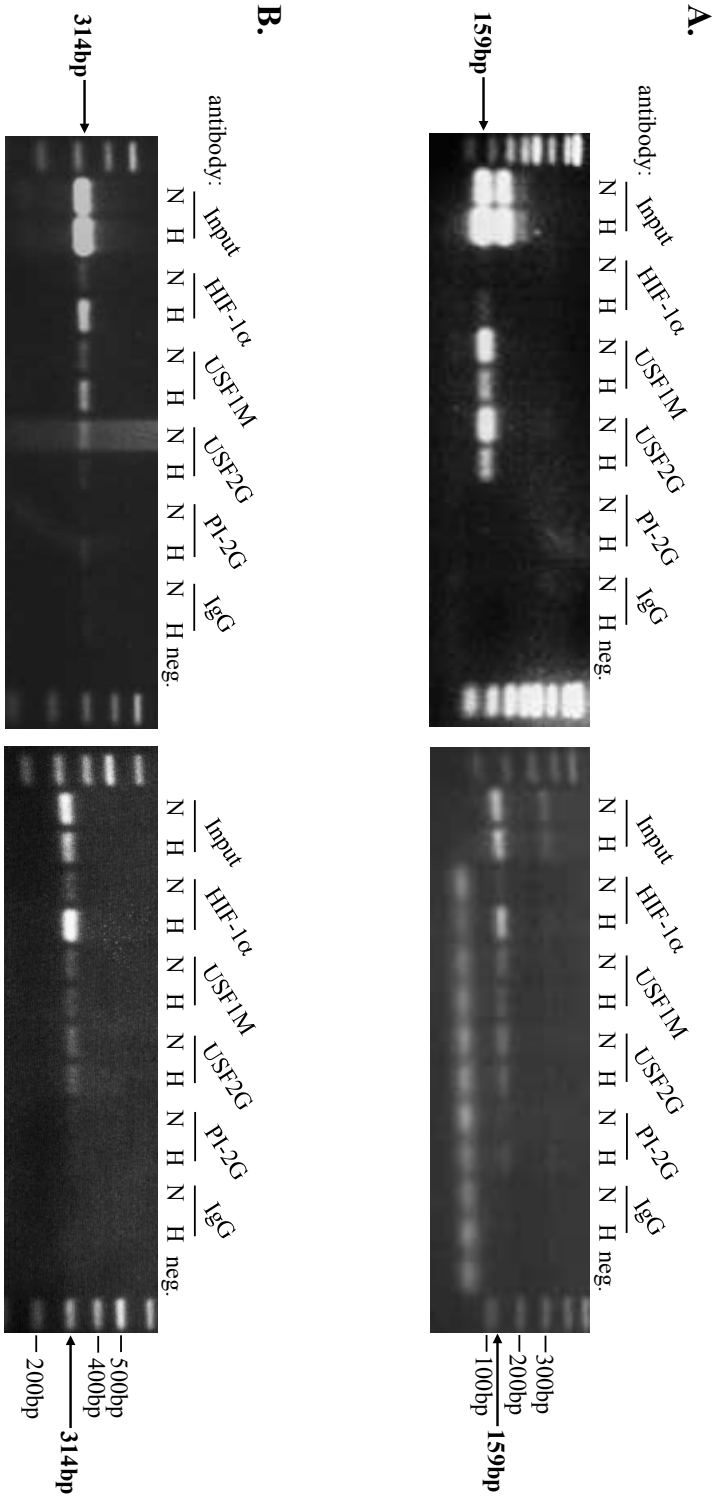

Hu et al. Figure 5

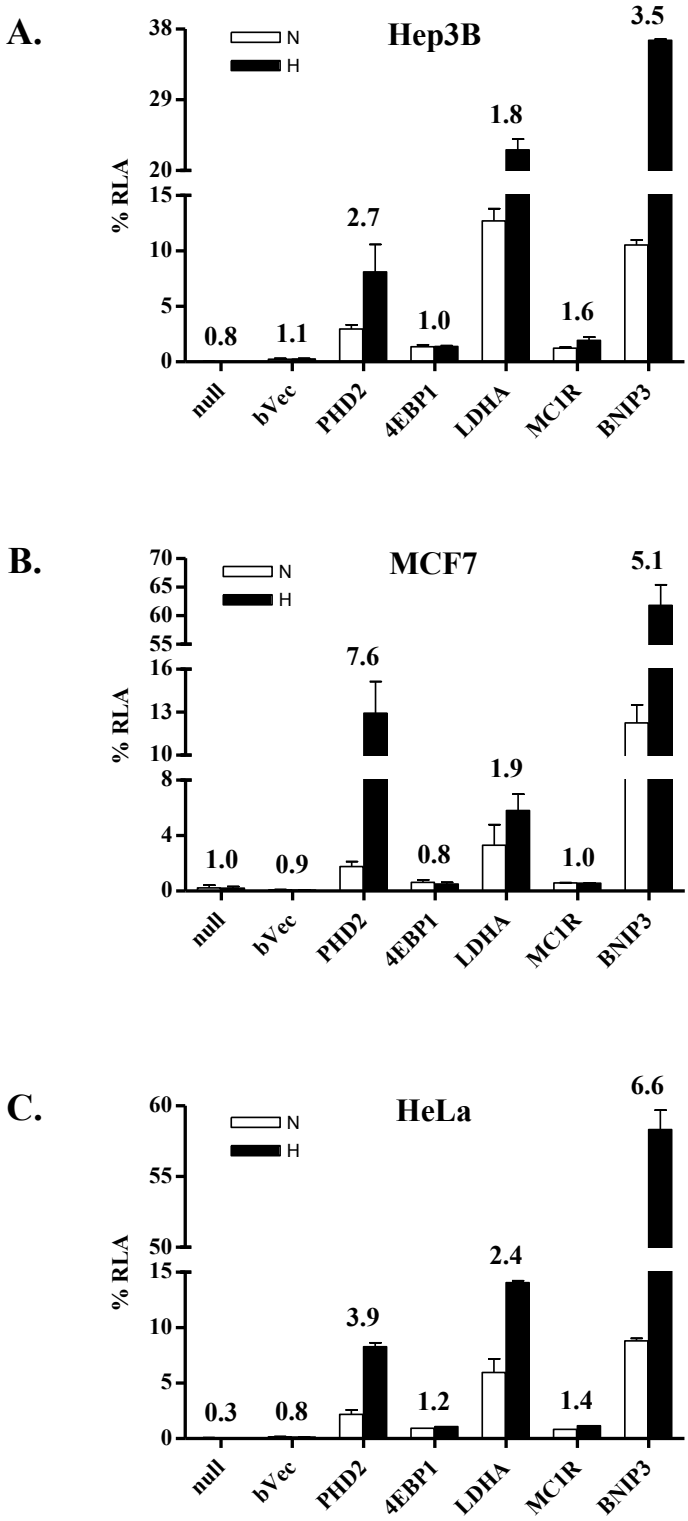

Hu et al. Figure 6

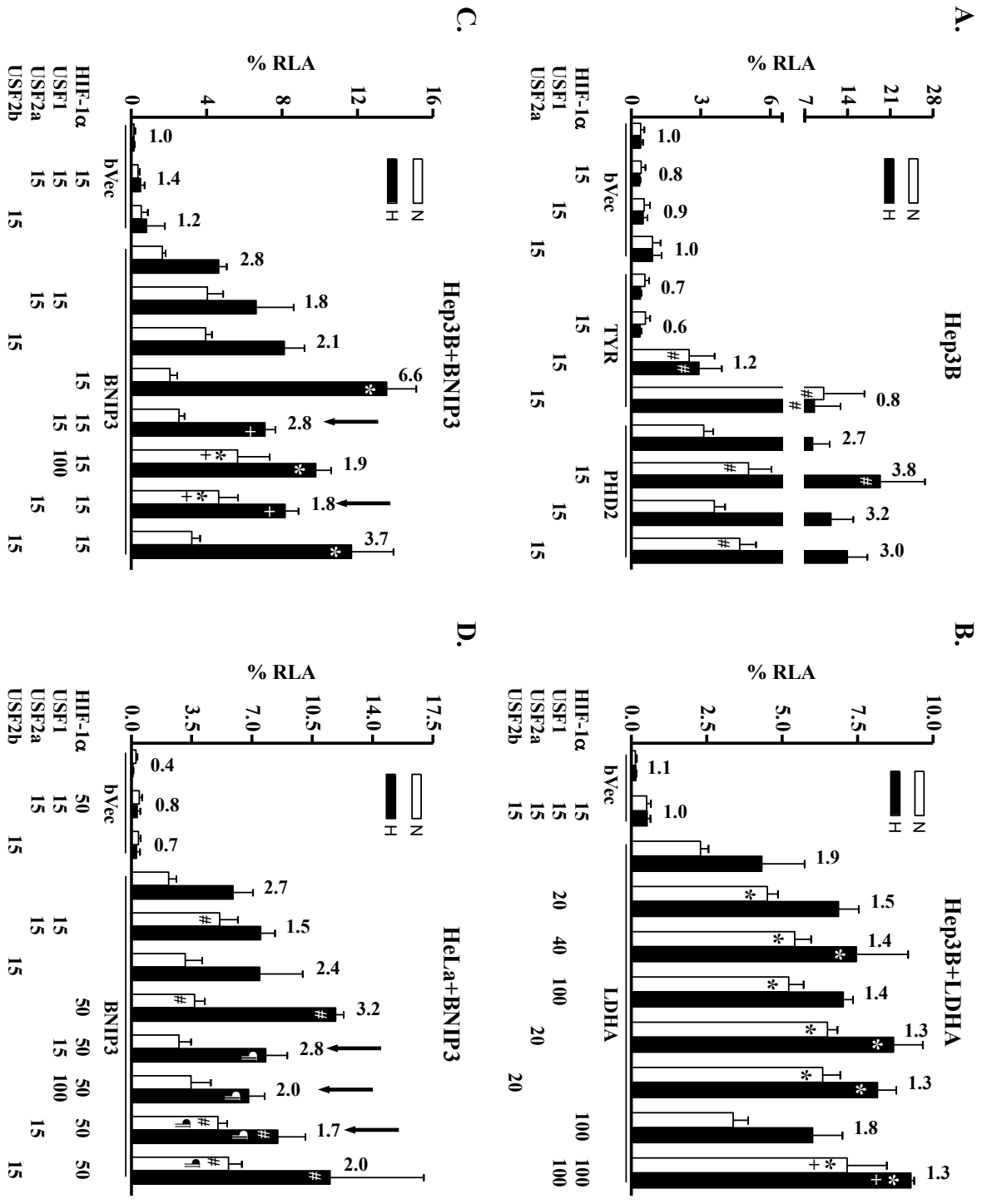

Hu et al. Figure 7

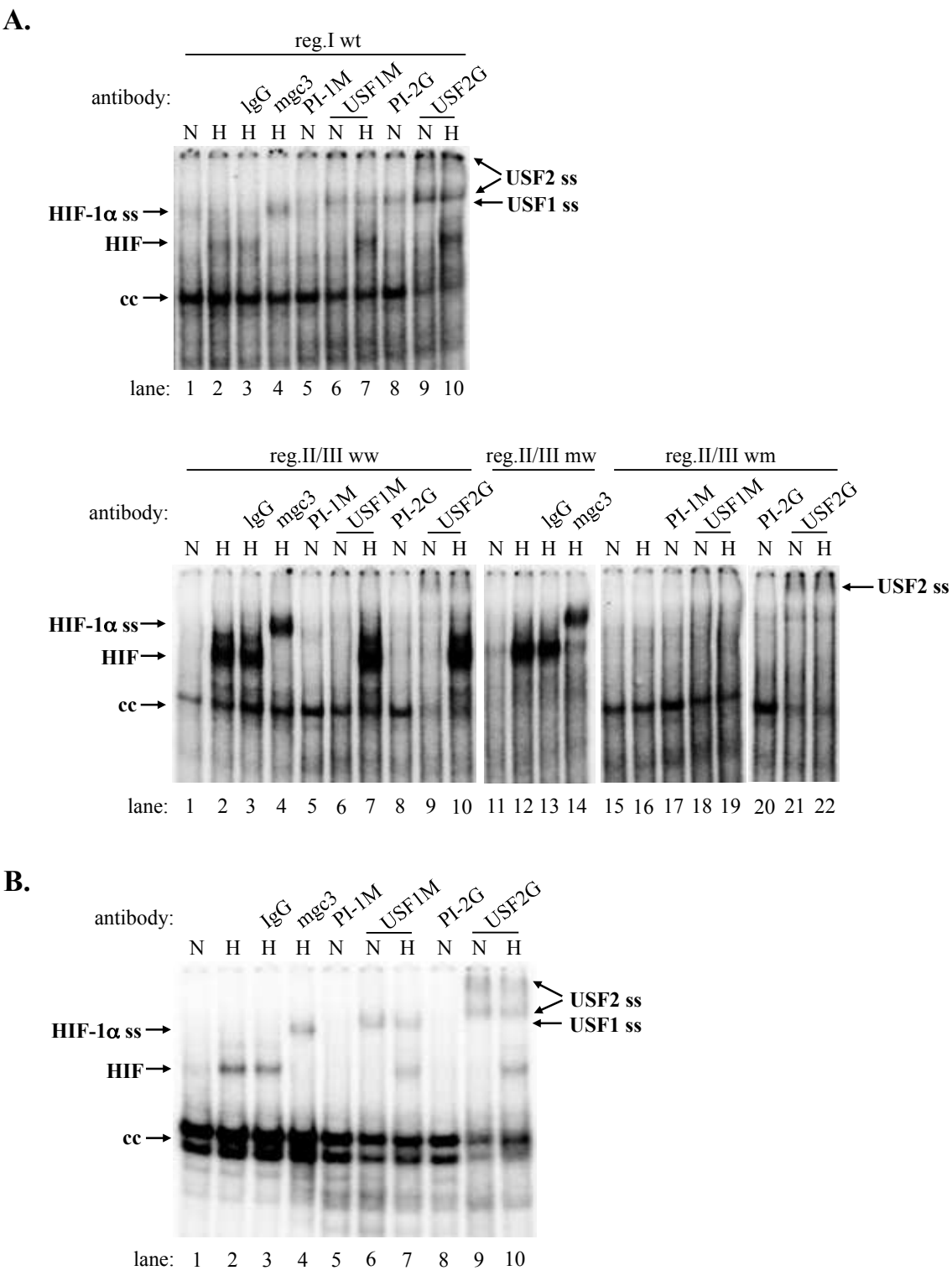

Supplement:

Interaction of HIF and USF signaling pathways at human genes flanked by hypoxia-response elements and E-box palindromes

Junmin Hu[1], Daniel P. Stiehl[2], Claudia Setzer[1], Daniela Wichmann[1], Dheeraj A. Shinde[1], Hubert Rehrauer[3], Pavel Hradecky[4], Max Gassmann[1,5], Thomas A. Gorr[1,6]

[1] Institute of Veterinary Physiology, University of Zurich, Zurich, Switzerland;

[2] Institute of Physiology, University of Zurich, Zurich, Switzerland;

[3] Functional Genomics Center Zurich, Zurich, Switzerland

[4] AltraBio, Lyon, France

[5] Zurich Center for Integrative Human Physiology (ZIHP), Zurich, Switzerland

[6] Center for Pediatrics and Adolescent Medicine, University Medical Center Freiburg, Freiburg, Germany

*** corresponding author:** Thomas A. Gorr, PhD

Institute of Veterinary Physiology, Vetsuisse Faculty, University of Zurich, Winterthurerstrasse 260, 8057 Zurich, Switzerland

💻 tgorr@access.uzh.ch ☎ +41 (0)44 635 8807 🖹 +41 (0)44 635 8932

Supplement Table ST1: PCR primers and oligonucleotides

PCR primers for generation of luciferase constructs (Fig. 5, 6)		
Name	For	Rev
4EBP1	F1: 5′-GTTGGTTCACTCCTCCTC-3′ F2: 5′-AGCATAACTACTCAATCCCC-3′	R1: 5′-CCAACAGATAATACCCATCC-3′ R2: 5′-CGTGTTTGTTAGGTGTCAG-3′
MC1R	F1: 5′-CTGAAAACACCAACCTCTCC-3′ F2: 5′-CTTTCACGCTCTGCCC-3′	R1: 5′-CCACACAATATCACCACCTC-3′ R2: 5′-CACAGCCATAGTCCTGTCC-3′
LDHA	F1: 5′-GAGTGGGAGCTGGTAGG-3′ F2: 5′-CAGGGATGAAGAAGAAACAG-3′	R1: 5′-GCTATCCAAGGCACAGG-3′ R2: 5′-TGAGATTTGAGTGGGAGAAC-3′
TYR	F1: 5′-TTGTAGCCTCTTTATGGTCTC-3′ F2: 5´CTCTATTCCTGACACTACCTCTC 3′	R1: 5′-TTATTTCCCAAACATTCCTG-3′ R2: 5′-CCAATTAGTCTGGGATAAGG-3′
pCRII	F1: 5′-CACACAGGAAACAGCTATGAC-3′	
LDHA/pCRII		R1: 5′-GATAAGCTTTAGAGGATGGGGTCAAGG-3′

Oligonucleotide sequences used for EMSA and pull-down experiments (Fig. 1, 7) Binding motifs, HREs or E-box, are underlined + in bold; h = human		
Name	Sense	Antisense
Daphnia phb2 w-146HRE	5′-GAACCATA**CACGTG**CCTCGAGCAG-3′	5′-CTGCTCGAGGCACGTGTATGGTTC-3′
Daphnia phb2 m-146HRE	5′-GAACCATA**CAATGT**CCTCGAGCAG-3´	5′-CTGCTCGAGGACATTGTATGGTTC-3′
Daphnia phb2 w-107HRE	5′-ACACGGCC**TACGTG**ATGATAGCGC-3′	5′-GCGCTATCATCACGTAGGCCGTGT-3′
Daphnia phb2 m-107HRE	5′-ACACGGCC**TAATGT**ATGATAGCGC-3′	5′-GCGCTATCATACATTAGGCCGTGT-3′
hBNIP3 HRE wt	5′-ACGCGCCG**CACGTG**CCACACGCAC-3′	5′-GTGCGTGTGGCACGTGCGGCGCGT-3′
hBNIP3 HRE mut	5′-ACGCGCCG**CAATGT**CCACACGCAC-3′	5′-GTGCGTGTGGACATTGCGGCGCGT-3′
hLDHA reg.I wt	5′-TCCCAGCG**CACGTG**GAGCAGTCTG-3′	5′-CAGACTGCTCCACGTGCGCTGGGA-3′
hLDHA reg.I mut	5′-TCCCAGCG**CAATGT**GAGCAGTCTG-3′	5′-CAGACTGCTCACATTGCGCTGGGA-3′
hLDHA reg.II/III ww	5′-CGACTCA**CACGTG**GGTTCCCG**CACGTC**CGCCGGC-3′	5′-GCCGGCGGACGTGCGGGAACCCACGTGTGAGTCG-3′
hLDHA reg.II/III mw	5′-CGACTCA**CAATGT**GGTTCCCG**CACGTC**CGCCGGC-3′	5′-GCCGGCGGACGTGCGGGAACCACATTGTGAGTCG-3′
hLDHA reg.II/III wm	5′-CGACTCA**CACGTG**GGTTCCCG**ACATTC**CGCCGGC-3′	5′-GCCGGCGGAATGTCGGGAACCCACGTGTGAGTCG-3′
hLDHA reg.II/III mm	5′-CGACTCA**CAATGT**GGTTCCCG**ACATTC**CGCCGGC-3′	5′-GCCGGCGGAATGTCGGGAACCACATTGTGAGTCG-3′

Primers for chromatin immunoprecipitation (ChIP) (Fig. 4)		
Name	For	Rev
LDHA	5′-ACTCAGGCTCATGGCTC-3′	5′-GGCTGGGGGTGGATG-3′
BNIP3 HRE	5′-TAGCCAGTGCCCAGAGAGTCC-3′	5′-ATTGGCCGCGACTTGGG-3′

siRNA oligonucleotides for transient knockdown HIF-1α, USF1 and USF2a in Hep3B cells (Fig. 2, 3)				
Gene	Sense	Antisense	Genbank accession No.	Targeted region
HIF-1	5′-CUGAUGACCAGCAACUUGAdTdT-3′	5′-UCAAGUUGCUGGUCAUCAGdTdT-3′	AF304431.1	1380-1400
USF1	5′-GACCCAACCAGUGUGGCUAdTdT-3′	5′-UAGCCACACUGGUUGGGUCdTdT-3′	NM_007122	79-97
USF2a	5′-UCCAGACUGUAACGCAGACAAdTdT-3′	5′-UUGUCUGCGUUAACAGUCUGGAdTdT-3′	NM_003367	786-806

Primers for real-time quantitative PCR (qPCR) of following human transcripts (Fig. 3)		
Name	For	Rev
LDHA	F2: 5′-GGAGATTCCAGTGTGCCTGT-3′	R2: 5′-GTCCAATAGCCCAGGATGTG-3′
BNIP3	F2: 5′-AGGGCTCCTGGGTAGAACTG-3′	R2: 5′-CCCTGTTGGTATCTTGTGGTG-3′
BNIP3L	F2: 5′-GGCAATGGGAAAAATGGG-3′	R2: 5′-TCAAAGCCTCGACTTCCTTC-3′
4E-Bp1	F2: 5′-CGGGGACTACAGCACGAC-3′	R2: 5′-CCGCTTATCTTCTGGGCTATT-3′
VEGFC	F4: 5′-AAACAAGGAGCTGGATGAAGAG-3′	R4: 5′-GGATTTAGGGGTTGATTTCTGG-3′
L28	F1: 5′-GCAATTCCTTCCGCTACAAC-3′	R1: 5′-TGTTCTTGCGGATCATGTGT-3′

Fig. S1: USFs bind preferentially to the -146 palindrome and HIF-1 to the -107 HRE of *Daphnia's* hb2 promoter

Additional evidence for the interaction of USFs with the -146 phb2 CACGTG palindrome was obtained by adding increasing volumes of anti-USF1M (left) and anti-USF2G (right) antiserum into the binding reaction with nuclear extracts from normoxic (N) and hypoxic (H) Hep3B cells. The intensity of the constitutive CACGTG complex (cc) was observed to be reduced in a dose-dependent manner. In contrast, addition of the maximal volume of pre-immune serum (PI-1M and PI-2G) left the complex's intensity unaffected. As can be seen, binding of USF complexes to the -146 phb2 E-box is oxygen-independent (Fig. S1A). An earlier work had established the following isoform-specificity of each of the anti-USF antisera used: anti-USF1M serum recognizes USF1 (domain M), anti-USF2G recognizes USF2a or 2b (domain G) and anti-USF2aO recognizes USF2a (domain O) (1). Equipped with this knowledge, we were able in additional supershift experiments (not shown) to delineate the slightly different mobility of bands within the CACGTG-bound constitutive complex (Fig. S1A; cc) as summarized here: USF1/2 heterodimers (i.e. USF1/2a, USF1/2b, fast complex, "1/2"), 1/1 homodimers (medium complex, "1/1") or 2/2 homodimers (slow complex, "2/2") (Fig. S1A; see also (1)).

Our initial report on the regulation of *Daphnia* globin gene 2 (hb2) had shown that the asymmetric TACGTG elements at positions -258 and -107 of the promoter were absolutely necessary for the hypoxic induction of the hb2 gene (2). To test whether these two sites indeed comprise avid HIF binding sequences (i.e. are HREs), we applied the pull-down assay with beads coated either with wildtype -107 HRE or -146 E-box oligonucleotides for a relative comparison of HIF's in vitro binding affinity. As can be seen in Fig. S1B, the amount of pulled HIF-1α protein left attached to the beads in the competed reactions (50× comp.) clearly demonstrates HIF's hypoxia-induced, high-affinity interaction with the -107 HRE and low-affinity interaction with the -146 palindromic E-box. In contrast, USFs display opposite in vitro binding behavior, with a tight interaction of USF2a and 2b to the -146 E-box and a weak, easily competed one to the -107 HRE (note 50x comp. lanes in Fig. S1C).

The pull-down assay thus demonstrates the opposite binding preferences of USF1/2 (primarily to CACGTG motif) versus HIF-1 complexes (primarily to TACGTG HRE) within the phb2 DNA in confirmation of our previous observations (2).

To assess whether the observed (2) USF-HIF interference in phb2 results from a direct or indirect contact between these transcription complexes, we conducted bidirectional co-immunoprecipitation (Co-IP) experiments. Positive Co-IP controls clearly confirmed precipitation (IP lanes), hence physical contact, between HIF-1α with immobilized ARNT (Fig. S1D), or conversely, ARNT with immobilized HIF-1α upon the subunits accumulation in hypoxic (H) extracts (Fig. S1E). As expected, the minuscule amount of HIF-1α present in normoxic (N) extracts is reflected by a small quantity of pulled ARNT protein (Fig. S1E left). However, neither immobilization scheme for the HIF-1α or HIF-1β (ARNT) subunit resulted in any detectable precipitation of USF2a (Fig. S1D and E right). Lack of co-immunoprecipitation suggests the absence of any physical interaction between HIF-1α or ARNT with USFs. Rather, the USF-HIF interference seems to be DNA context dependent.

Hu et al. Suppl. Figure 1

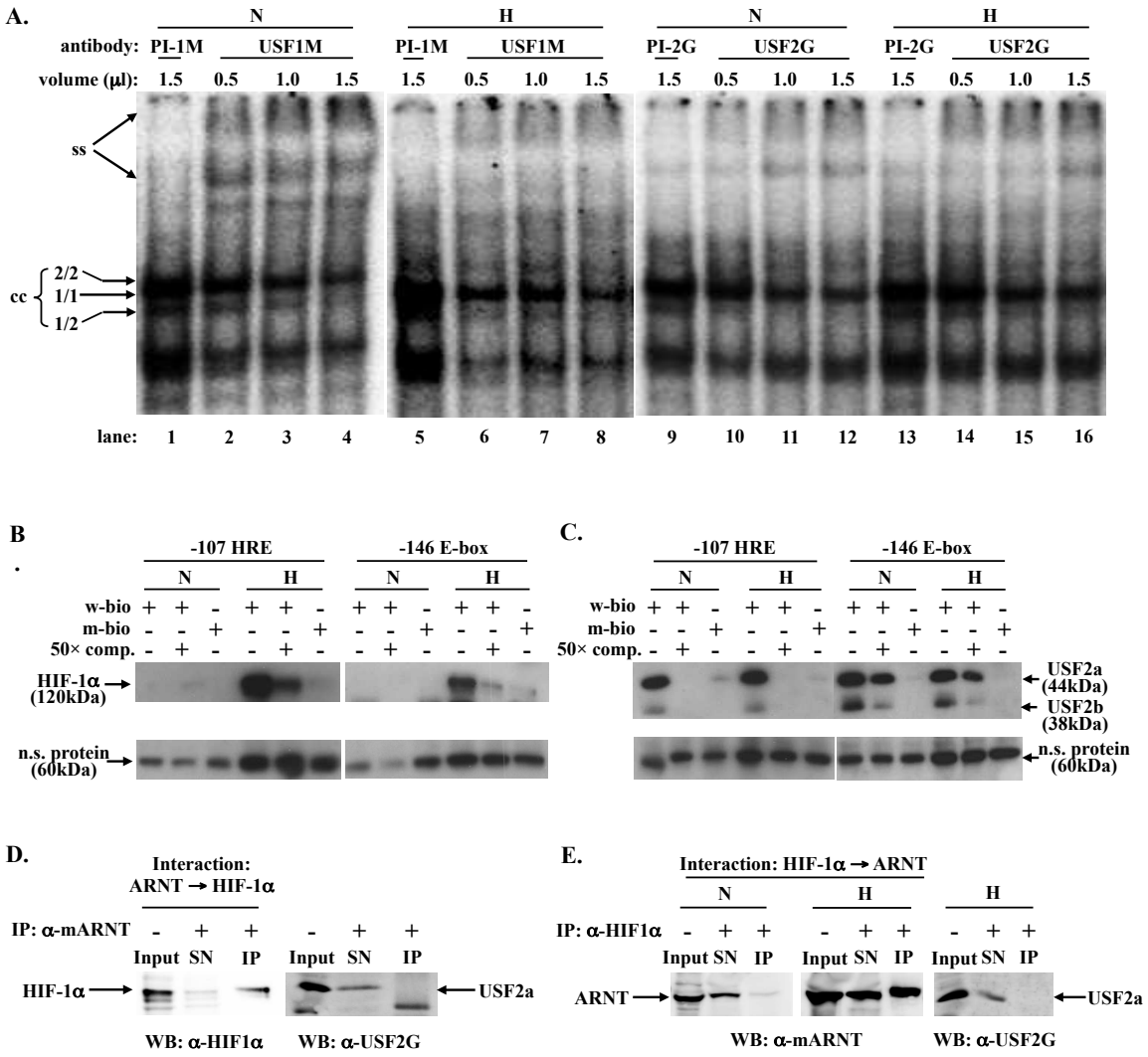

Suppl. Fig. S1. Protein-DNA and protein-protein interactions in the phb2 promoter (A) Dose dependent gel supershift with normoxic and hypoxic nuclear extracts from Hep3B cells by applying increasing volume of anti-USF1M or USF2G IgGs into the binding reaction as indicated. Representative PIs were used as negative controls. cc: constitutive CACGTG complex; ss: supershifted CACGTG complex**.** (B and C) Pull-down analysis either with -107 HRE wild type oligonucleotides (-107 HRE: 5'-TACGTG-3') or with -146 E-box wild type biotinylated oligonucleotides (-146 E-box: 5'-CACGTG-3') using HeLa normoxic and hypoxic nuclear protein. (B) HIF-1α detection with anti-HIF-1α antibody (mgc3); (C) USF2a/2b detection with anti-USF2G antibody. Staining of non-specific (ns) proteins indicated as loading control. (D) HIF-1α (left) or USF2a (right): Western blot of extracts immunoprecipitated (IP) by anti mouse ARNT IgG compared to non-precipitated supernatants (SN). (E) ARNT (left) or USF2a (right): Western blot of extracts imunoprecipitated (IP) by anti HIF-1α IgG compared to non-precipitated supernatants (SN). Input: only nuclear extract (25μg); SN: supernatant from IP; IP: immunoprecipitation fraction, N: normoxia (air); H: hypoxia, 1% O_2 16h.

Supplement Fig. S2: Human genes selected for HIF or USF control and HIF/USF co-targeted reporter constructs

Sequence analysis (see text, Table 2) and promoter alignment revealed human-mouse-rat (hmr) conservation of HREs and/or E-box palindromes in the promoters of the following control (a+b) and HRE/E-box candidate genes (c-f) Alignment examples are presented here only for TYR, PHD2, LDHA and BNIP3 promoter regions (Fig. S3):

a) human tyrosinase (TYR): USF specific target gene with two hmr conserved CATGTG E-boxes (-183/-178 and -91/-86). E-box (-183/-178) validated as direct binding site for USF1 (3).

b) human prolyl hydroxylase domain 2 (PHD2): HIF-1 specific target gene with hm conserved HRE (-413/-408) as functional HIF-1 binding site (4).

c) human 4E-binding protein 1 (4EBP1): contains hmr conserved E-box palindrome (-179/-174) and non-conserved HRE candidate (-123/-115).

d) human lactate dehydrogenase A (LDHA): contains distinct, hmr conserved CACGTG palindrome (region II -2367/-2362) and CACGTC site (region III -2353/-2348; reads as reverse-complement: GACGTG) as well as another CACGTG E-box (region I -2465/-2460) with hm conservation. Region I and II: validated MYC binding sites (5). Region II and III: validated in vitro HIF-1 binding sites (6).

e) human melanocorticotropin 1 receptor (MC1R): contains two E-boxes, one of which with hm conservation (-461/-456) whose role in controlling MC1R expression in response to UVB (80mJ/cm^2) is known thanks to the work of Corre et al. (3) .

f) human BCL2/E1B 19 kDa interacting protein 3 (BNIP3): contains hmr conserved HRE (-251/-246), a validated functional HIF-1 site (7), which is identical to E-box palindrome.

Suppl. Fig. S2 Mouse-rat-human alignments of relevant HRE, E-box palindrome or HRE/E-box containing promoter regions for genes TYR, PHD2, LDHA and BNIP3. TYR with two hmr conserved CATGTG E-boxes (italics + underlined). PHD2 with known functional HRE (underlined). LDHA with known functional HRE (underlined) and E-box palindromes (italics + underlined). BNIP3 with known functional HRE (underlined).

Hu et al. Suppl. Figure 3

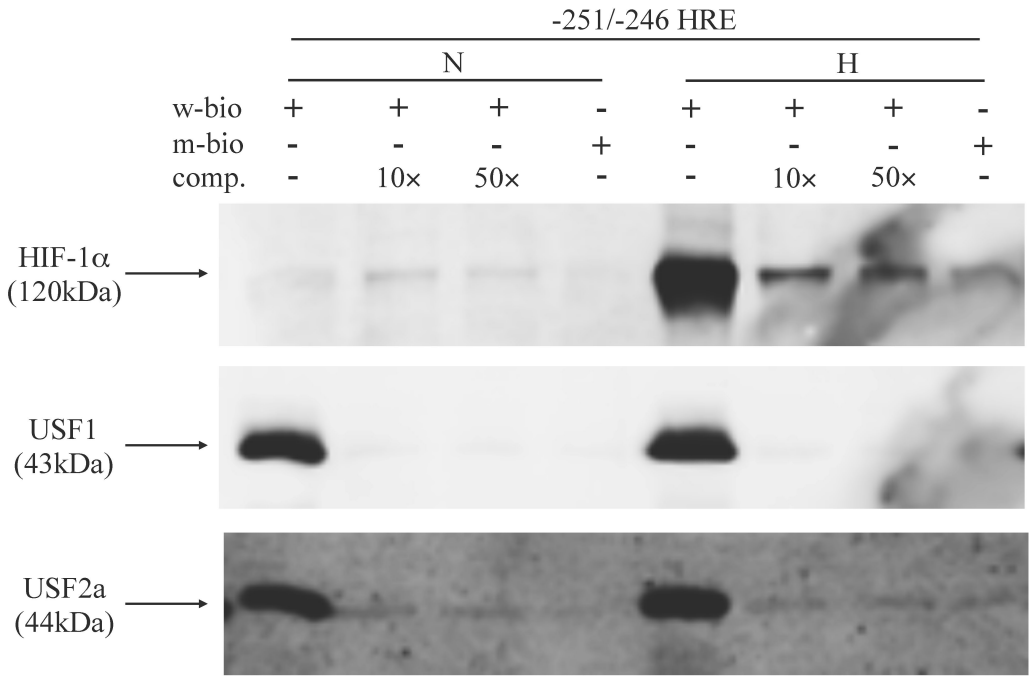

Suppl. Fig. S3: Pull-down analysis with human BNIP3 biotinylated wildtype -251/-246 HRE oligonucleotide using Hep3B normoxic (N) and hypoxic (H) nuclear extracts. Binding specificity was assessed either through beads coated with mutant (m-bio) HRE (5'-CAATGT-3') or with binding reactions containing 10- or 50-fold molar excess of free wildtype oligonucleotide as competitor (comp.). Oligonucleotide sequences: see Suppl Table ST1 (hBNIP3 HRE wt, hBNIP3 HRE mut). Immunoblots of bound factors were performed with mouse anti-HIF1α (upper panel); anti-USF1 (C-20) (middle panel) and anti-USF2G (lower panel). Results reproduced in n = 3-4 independent assays.

References in Supplement

1. Viollet B, Lefrancois-Martinez AM, Henrion A, Kahn A, Raymondjean M, Martinez A. Immunochemical characterization and transacting properties of upstream stimulatory factor isoforms. J Biol Chem. 1996;271:1405-15.

2. Gorr TA, Cahn JD, Yamagata H, Bunn HF. Hypoxia-induced synthesis of hemoglobin in the crustacean Daphnia magna is hypoxia-inducible factor-dependent. J Biol Chem. 2004;279:36038-47.

3. Corre S, Primot A, Sviderskaya E, Bennett DC, Vaulont S, Goding CR, et al. UV-induced expression of key component of the tanning process, the POMC and MC1R genes, is dependent on the p-38-activated upstream stimulating factor-1 (USF-1). J Biol Chem. 2004;279:51226-33.

4. Metzen E, Stiehl DP, Doege K, Marxsen JH, Hellwig-Burgel T, Jelkmann W. Regulation of the prolyl hydroxylase domain protein 2 (phd2/egln-1) gene: identification of a functional hypoxia-responsive element. Biochem J. 2005;387:711-7.

5. Shim H, Dolde C, Lewis BC, Wu CS, Dang G, Jungmann RA, et al. c-Myc transactivation of LDH-A: implications for tumor metabolism and growth. Proc Natl Acad Sci U S A. 1997;94:6658-63.

6. Semenza GL, Jiang BH, Leung SW, Passantino R, Concordet JP, Maire P, et al. Hypoxia response elements in the aldolase A, enolase 1, and lactate dehydrogenase A gene promoters contain essential binding sites for hypoxia-inducible factor 1. J Biol Chem. 1996;271:32529-37.

7. Kothari S, Cizeau J, McMillan-Ward E, Israels SJ, Bailes M, Ens K, et al. BNIP3 plays a role in hypoxic cell death in human epithelial cells that is inhibited by growth factors EGF and IGF. Oncogene. 2003;22:4734-44.